Clusters and correlations in nuclear structure and reactions

ZOOM with Tongji University - Shanghai - 25 Nov 2021

Lorenzo Fortunato
Univ. Padova & INFN
Italy

name	shape	group	Γ_{vib}	Patterns
linear =		$\mathcal{D}_{\infty h}$	$A_{1g} + A_{1u} + E_{1u}$	
linear $\neq$		$\mathcal{C}_{\infty \nu}$	$2A_1 + E_1$	
equilateral		$\mathcal{D}_{3h}$	$A_1' + E'$	
isosceles		$\mathcal{C}_{2\nu}$	$2A_1 + B_1$	
scalene		$\mathcal{C}_s$	$3A'$	

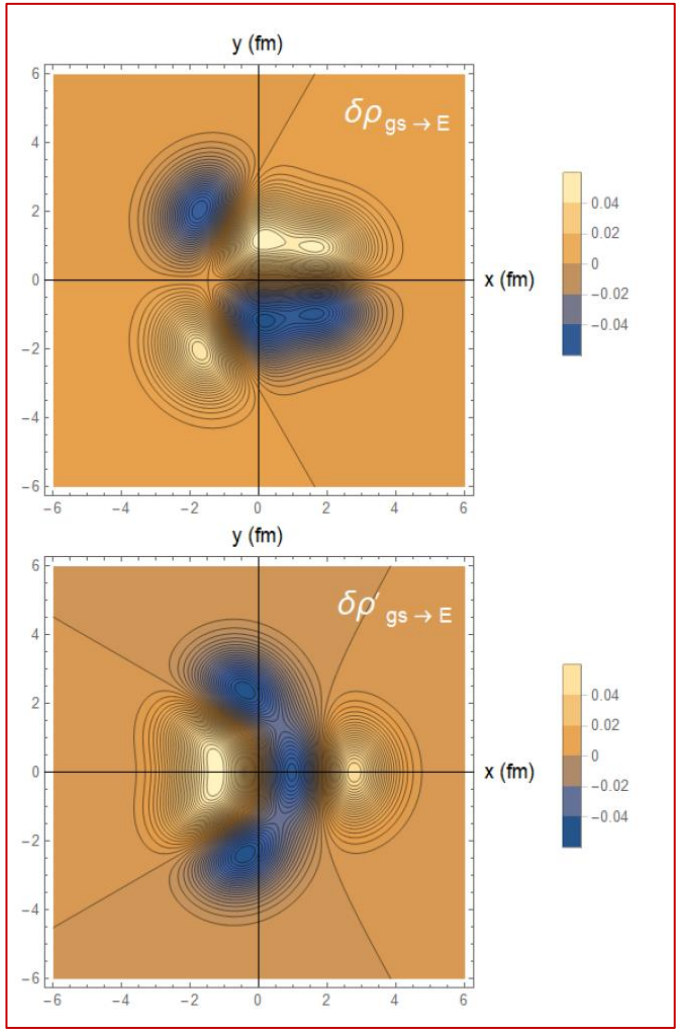

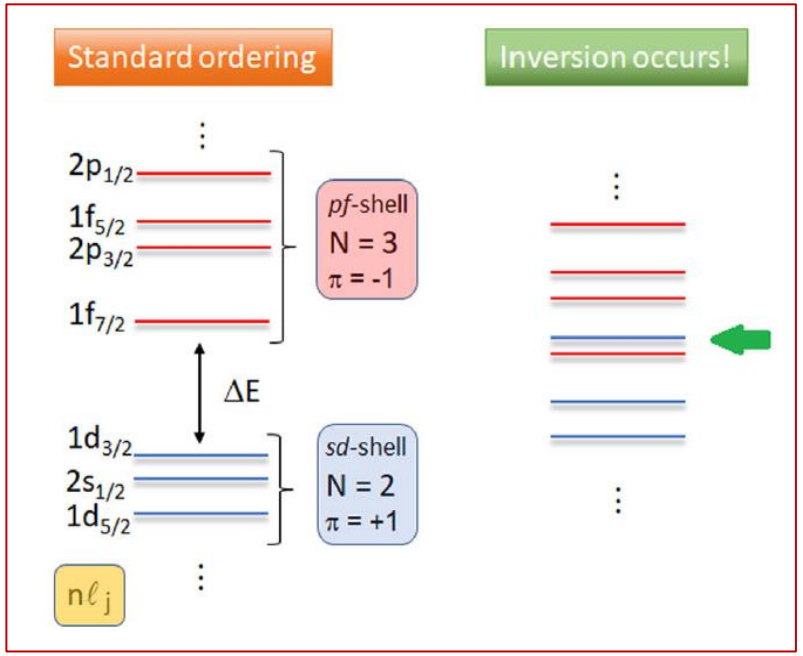

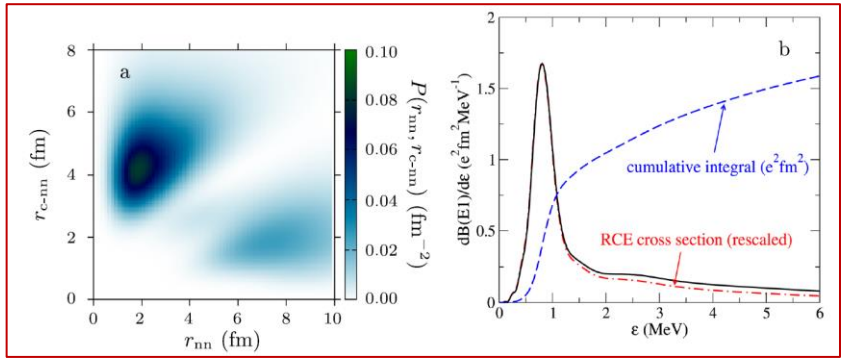

800 ANNI 1222·2022
UNIVERSITÀ DEGLI STUDI DI PADOVA
Dipartimento di Fisica e Astronomia Galileo Galilei
INFN Istituto Nazionale di Fisica Nucleare

Collaborators

L. Fortunato

Jesús Casal (Padova and now Seville)

Jagjit Singh (Padova, Sapporo and Osaka)

Wataru Horiuchi (Sapporo)

Andrea Vitturi (Padova)

Edoardo Lanza (Catania)

Oct. 2021

Outline of the presentation

- Polarized gamma beams: scenario for future measurements on the depolarization ratio for the case of 12C with triangular and more exotic structures

- Transition densities in action for 12C and 16O, recent results on alpha-transfer form factors

- New insight on the structure of 29F at the border of the island of inversion

Discrete symmetries and polarized gamma-rays in 12C

PHYSICAL REVIEW C **99**, 031302(R) (2019)

Rapid Communications | Editors' Suggestion

Establishing the geometry of α clusters in ^{12}C through patterns of polarized γ rays

Lorenzo Fortunato
Dipartimento di Fisica e Astronomia "G.Galilei"-Università di Padova, via Marzolo 8, I-35131 Padova, Italy and INFN-Sez.di Padova, via Marzolo 8, I-35131 Padova, Italy

(Received 13 December 2018; published 11 March 2019)

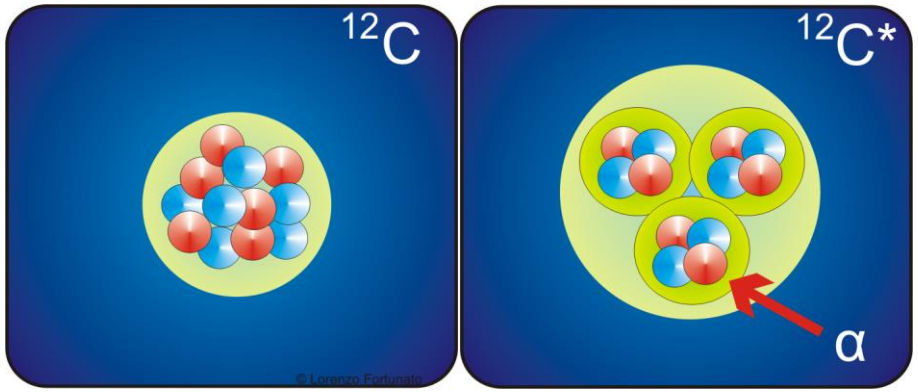

One can shoot linearly polarized gamma rays (Electric field oscillating in a given direction constant in time) of appropriate energy (tuned to match the resonances of interest) and observe the outcoming gammas of the same or different energies with a polarizer/analyzer. If the nucleus has a definite geometrical symmetry (i.e. if there is an underlying discrete group structure), very strict selection rules apply. Experimentally the polarization can be measured with another inverse Compton scattering.

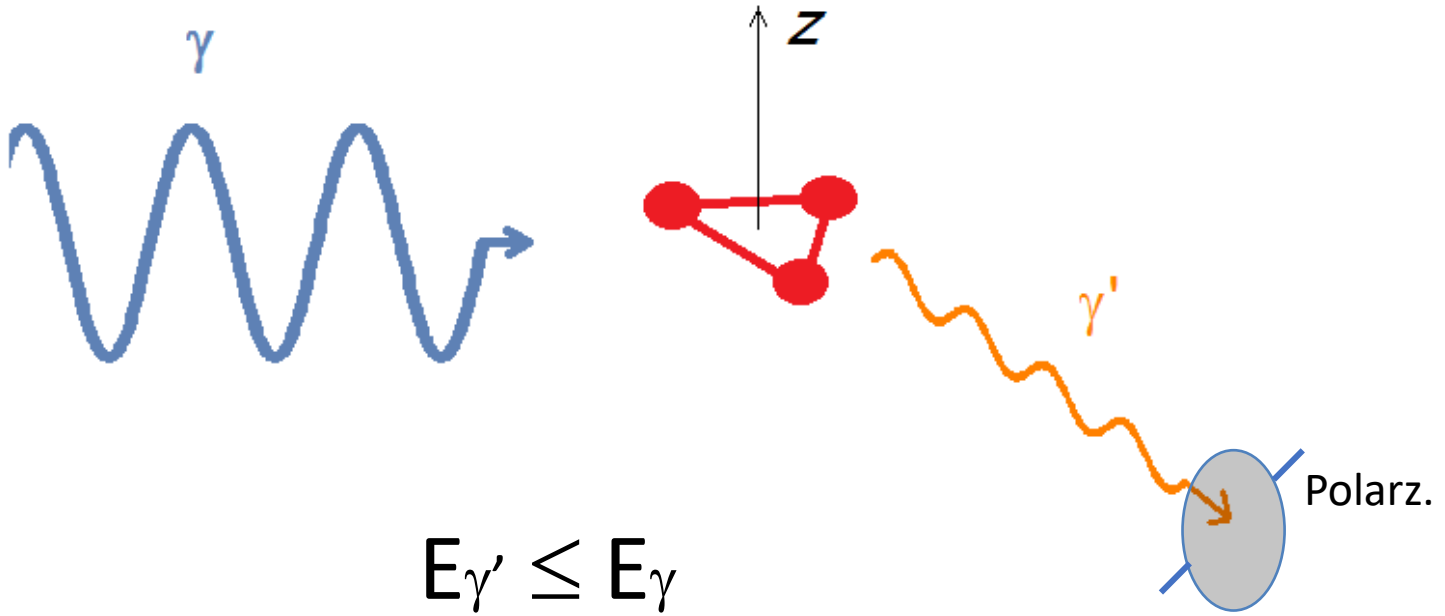

$E_{\gamma'} \leq E_{\gamma}$

Polarized gamma-ray facilites around the globe:

- Mainz Microtron MAMI (Continuous Wave, beam polarization 80%, En. resol. 0.1 MeV, but energy too high 50-800 MeV)
- Triangle University Higs facility (FEL type, quasi CW operation, 2-60 MeV, flux 10^8-10^9 phot./s)
- ELI-NP in Romania (0-20 MeV, high flux, high resolution, 100% polarization)
- LEPS – Japan (very high energy)
- NewSubaru
- …

Extreme Light Infrastructure
Nuclear Physics (ELI-NP)

Gamma beam parameter	Value
Energy [MeV]	0.2 – 19.5
Spectral density [ph/s/eV]	$0.8 - 4 \cdot 10^4$
Bandwidth rms [%]	≤ 0.5
#Photons/shot within FWHM bdw.	$\leq 2.6 \cdot 10^5$
#Photons/s within FWHM bdw.	$\leq 8.3 \cdot 10^8$
Source rms size [μm]	10 – 30
Source rms divergence [μrad]	25 – 200
Peak brilliance [N_{ph}/s·mm^2·mrad^2·0.1%bdw]	$10^{20} - 10^{23}$
Pulse length rms [ps]	0.7 – 1.5
Linear polarization [%]	> 99
Macro repetition rate [Hz]	100
Number of pulses/macropulse	32
Pulse–to–pulse separation [ps]	16

With the advent of the new facility in Romania, beams of high brilliance, focused, polarized gamma rays produced with Inverse Compton Scattering will become available with energies ranging from 0.2-20 MeV

Depolarization ratio

One can measure the so-called depolarization ratio between intensities, by turning the analyzer/polarizer of 90 degrees, i.e.:

$$\rho = \frac{I_{\perp}}{I_{\parallel}}$$

as a tool to determine which modes are totally symmetric modes. In fact from the theory of Raman scattering

$0 \leq \rho \leq \frac{3}{4}$ for polarized bands (symmetric modes)

$\rho = \frac{3}{4}$ for depolarized bands (non-symmetric modes)

even with a randomly oriented sample.

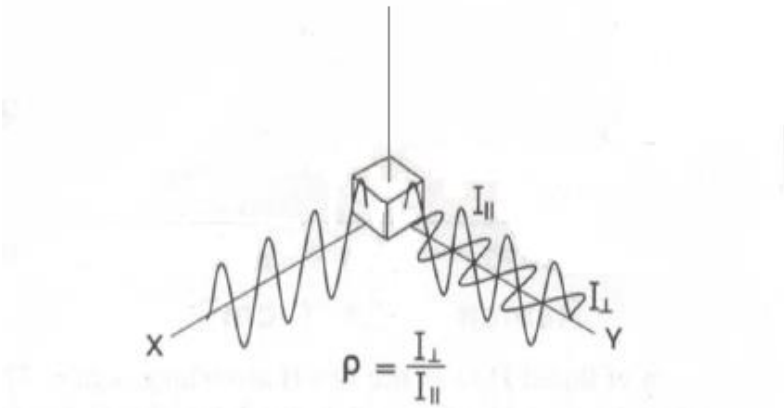

Figure 8.6. Parallel and perpendicular Raman scattering.

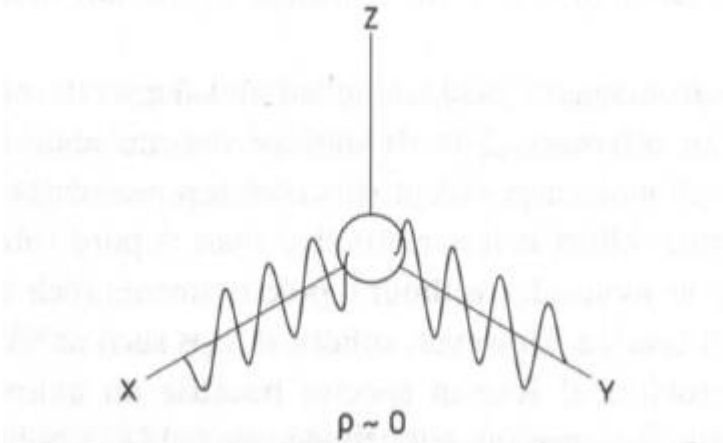

Figure 8.8. Polarized light scattering by a sphere.

Figures from book by P.Bernath

Depolarization ratio : a chemical example CCl_4

This kind of measuments of $\rho = \frac{I_\perp}{I_\parallel}$ are absolutely standard in optical spectroscopy (where polarizers and analyzers are easy to do and handle).

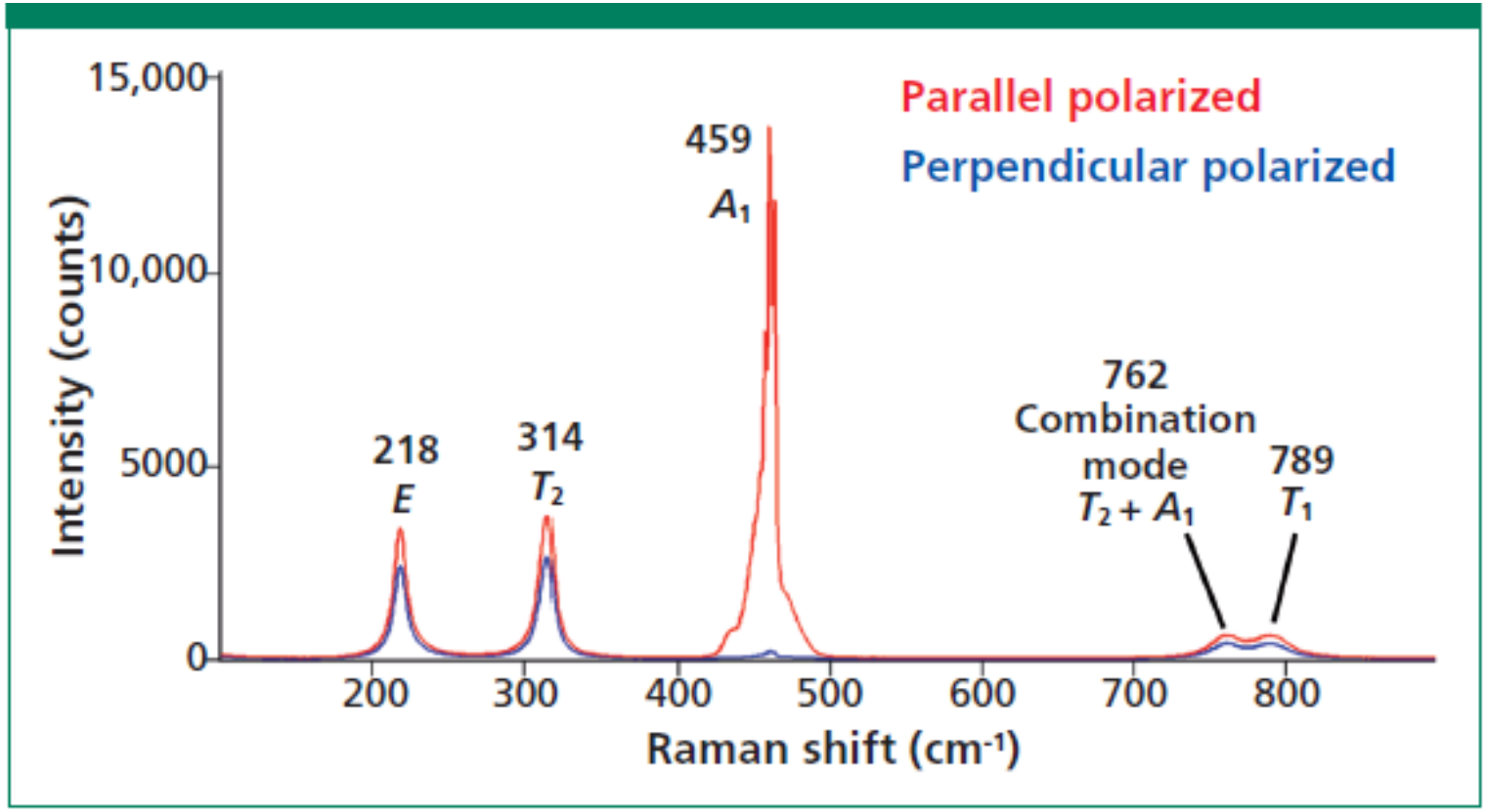

Figure 2: Polarized Raman spectra of CCl_4.

Figure from D.Tuschel – Spectroscopy (2014)

Depolarization ratio

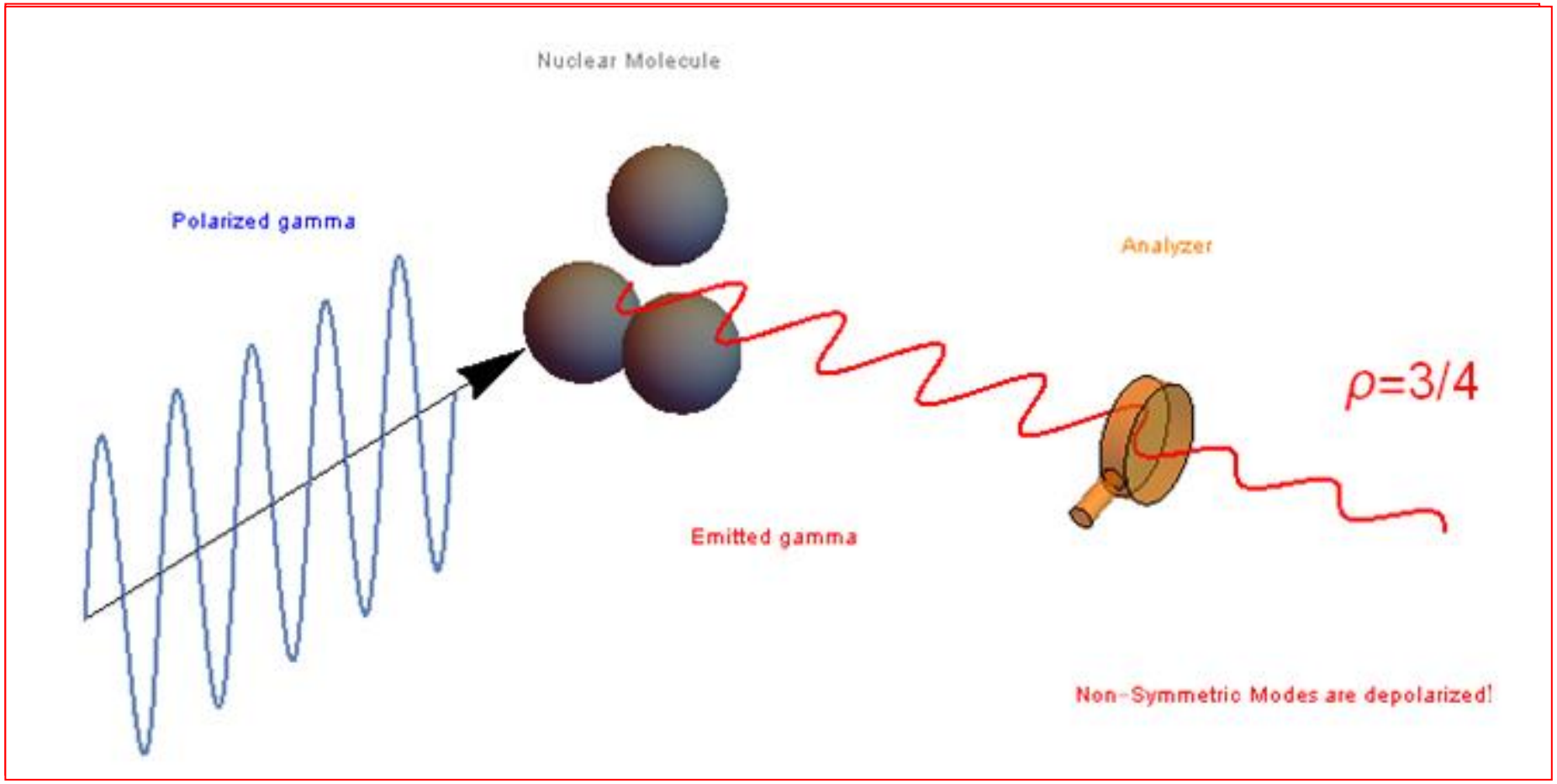

Panoply of different models … too many… just to name a few !!!

(Too) many models have been proposed for 12C where the triangle is not equilateral, isosceles, scalene or even a linear chain (Morinaga). Therefore. I have set forth to determine all possible outcomes and the patterns that can be predicted are intended as a guidance as to which configuration is right and **the crucial method is clearly through measurements of the depolarization ratio in Raman-like experiments of nuclear fluorescence** that will be feasible at ELI-NP or in other labs where gamma-rays are available.

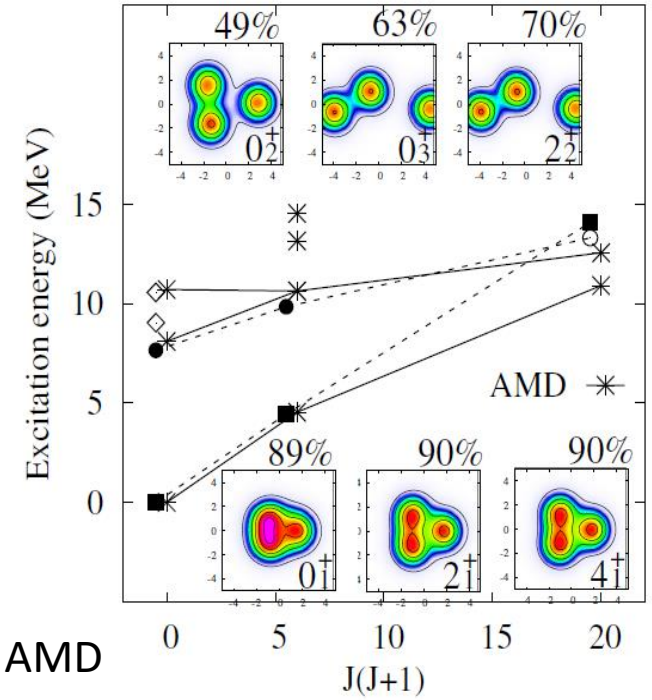

AMD

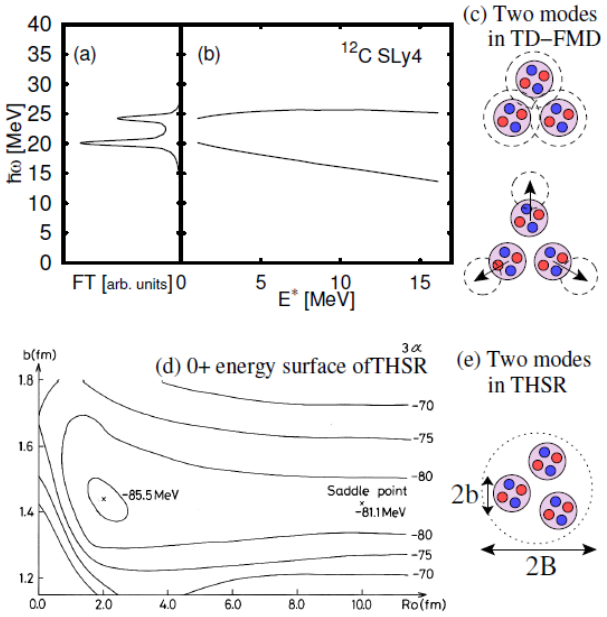

FMD

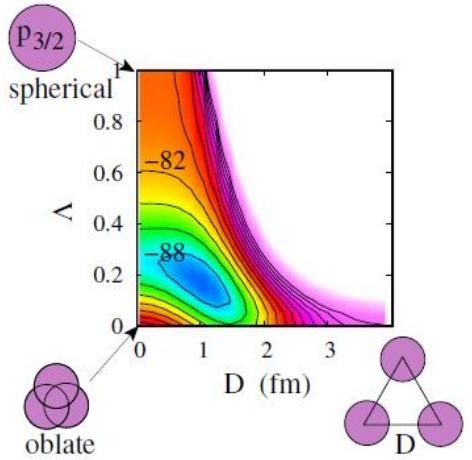

FIG. 10 (Color online) 0^+-projected energy surface on the Λ-D plane for ^{12}C calculated by the AQCM. The interaction and width parameters are same as those in Ref. (Suhara *et al.*, 2013).

antisymmetrized quasi-cluster model

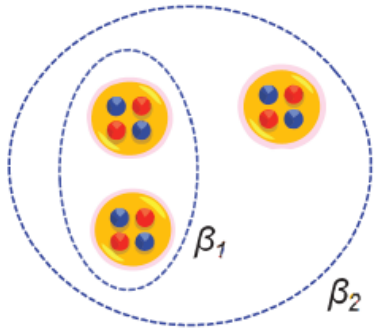

container model

Figures from: Freer et al. (2018) Microscopic clustering in Light Nuclei

Algebraic cluster model for 3 alphas

Bijker and Iachello (Ann.Phys. 298, 2002) have clearly demonstrated the succesfull application of the ACM, or algebraic cluster model, to the vibrational-rotational spectrum of alpha-conjugate nuclei like 12C and 16O.

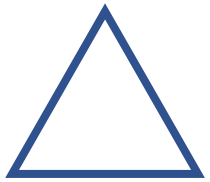

Note that rotational bands DO NOT conform tothe usual quadrupole rotational bands we are used, they have a different symmetry! Rather, these are the ways in which you can spin a triangle.

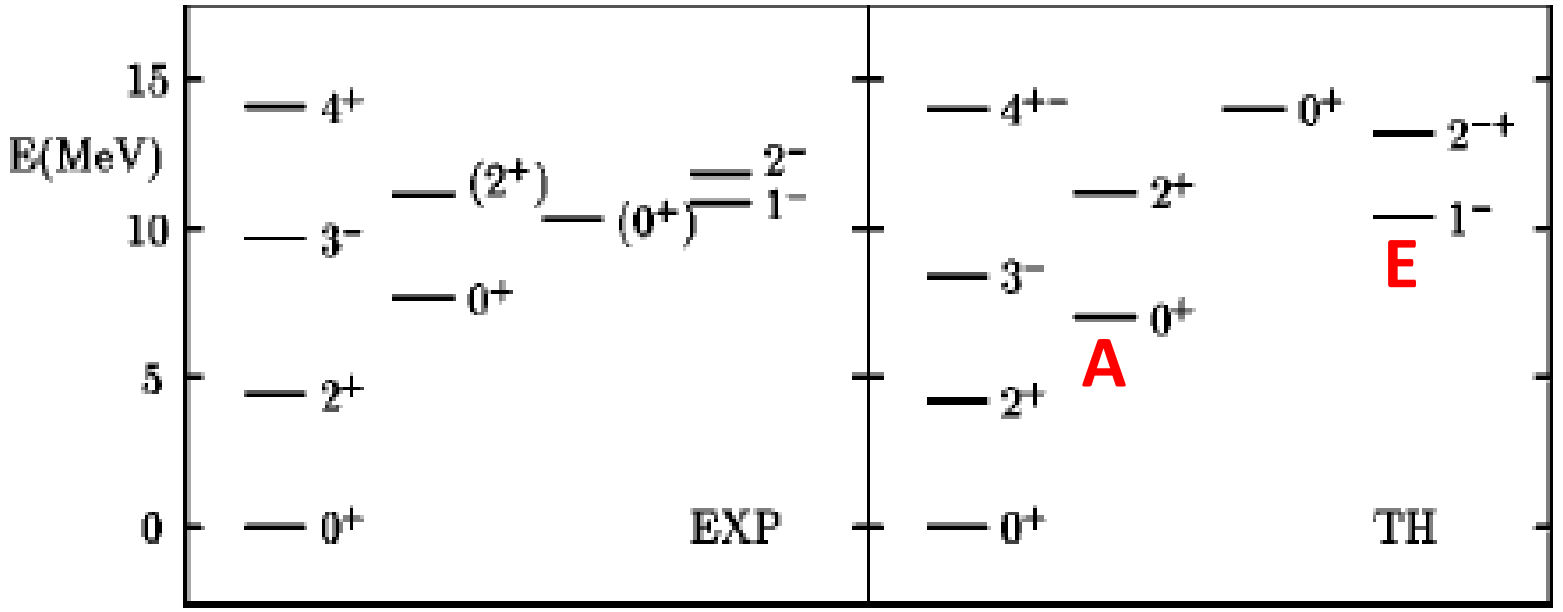

FIG. 2. Comparison between the low-lying experimental spectrum of ^{12}C [12] and that calculated using Eq. (6) with $A=7.0$, $B=9.0$, $C=0.7$, and $D=0.0$ MeV. States with uncertain spin-parity assignment are in parentheses.

PRL 113, 012502 (2014) PHYSICAL REVIEW LETTERS week ending 4 JULY 2014

Evidence for Triangular $\mathcal{D}_{3h}$ Symmetry in ^{12}C

D. J. Marín-Lámbarri,[1] R. Bijker,[2] M. Freer,[1] M. Gai,[3,4] Tz. Kokalova,[1] D. J. Parker,[1] and C. Wheldon[1]

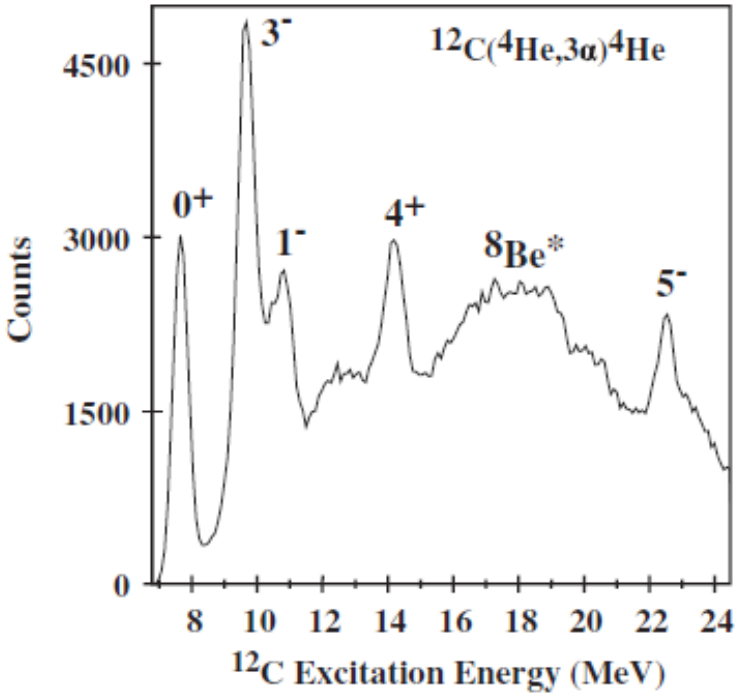

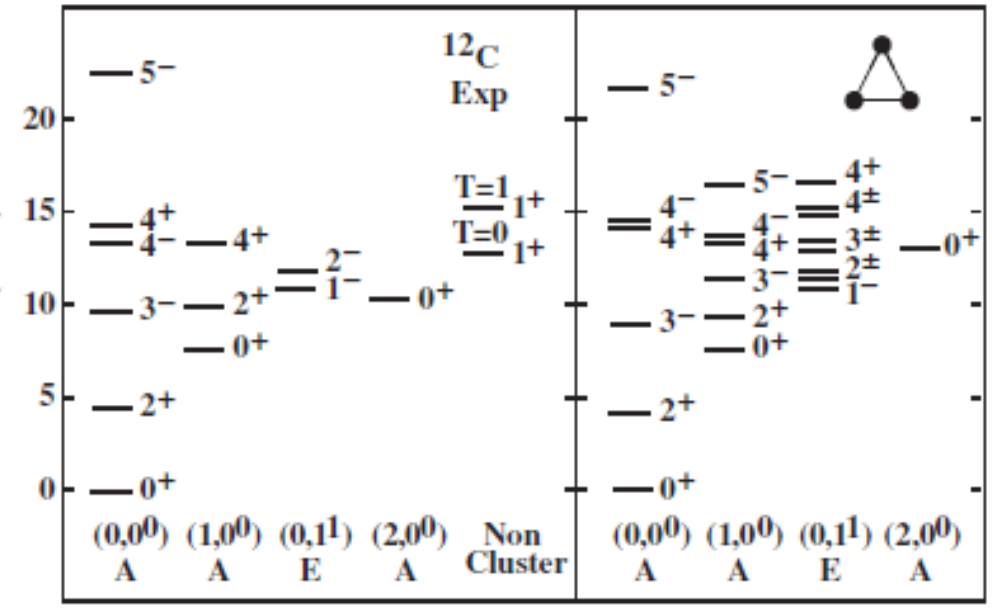

This lovely paper confirms the assignation of the 5- state at 22.4(2) MeV to the g.s. band of an **equilater triangular structure.**

Note the uncommon spin-parity of bands (the doublet 4+/ 4- has a natural explanation in terms of D3h symmetry!).

Working plan to implement this idea

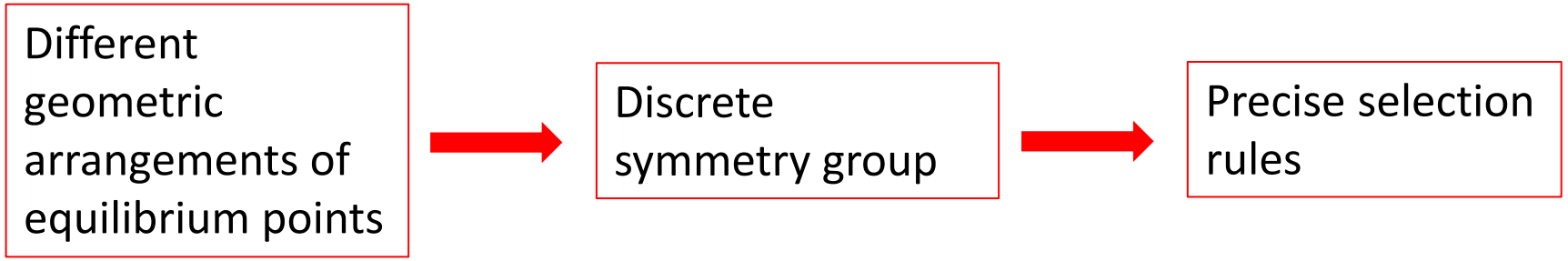

Work plan:

- Decide arrangement of N particles
- This means 3N-6 d.o.f (or 3N-5 d.o.f. for linear arrangement)
- Identify the underlying discrete group structure
- Find the character under transformations of the group Γ_{3N}
- Subtract translations and rotations to single out character of vibrational modes Γ_{vib}
- Identify patterns of totally symmetric modes
- Check models against measures of intensities $\rightarrow$ Eureka !!

Tables in PRC 99 (2019) paper: 3 equal clusters

name	shape	group	Γ_{vib}	Patterns
linear =		$\mathcal{D}_{\infty h}$	$A_{1g} + A_{1u} + E_{1u}$	
linear $\neq$		$\mathcal{C}_{\infty \nu}$	$2A_1 + E_1$	
equilateral		$\mathcal{D}_{3h}$	$A_1' + E'$	
isosceles		$\mathcal{C}_{2\nu}$	$2A_1 + B_1$	
scalene		$\mathcal{C}_s$	$3A'$	

The number of totally symmetric peaks over total is different in each case, therefore one can disentagle the various possibilities

Tables in PRC 99 (2019) paper

There might be more than just one configuration! The picture complicates a little, but not too much ! One can invoke the concept of descent in symmetry ans still apply some of the rules.

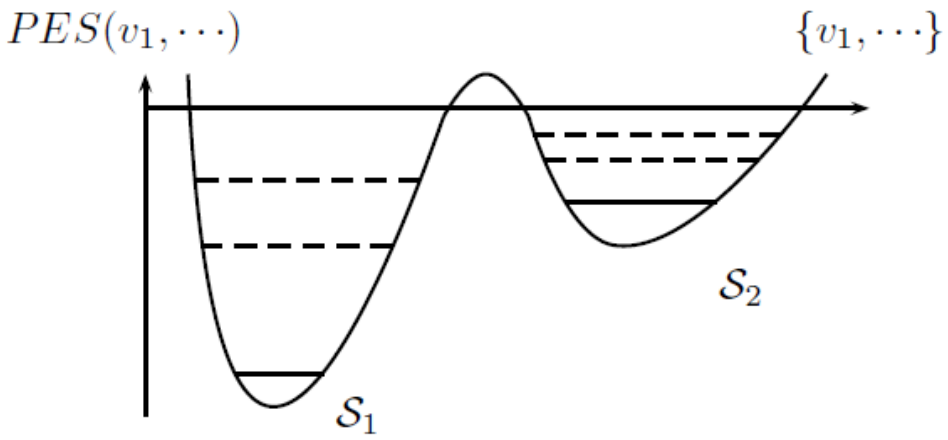

Group chains

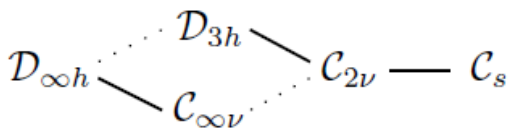

$\mathcal{D}_{\infty h}$	$A_{1g}+$	$A_{1u}+$	E_{1u}
$\mathcal{C}_{\infty\nu}$	A_1+	A_1+	E_1
$\mathcal{C}_{2\nu}$	A_1+	A_1+	$B_1 + B_2$
$\mathcal{C}_s$	$A'+$	$A'+$	A'

$\mathcal{D}_{\infty h}$	$A_{1g}+$	$A_{1u}+$	E_{1u}
$\mathcal{D}_{3h}$	$A_1'+$	$A_2''+$	E'
$\mathcal{C}_{2\nu}$	A_1+		$A_1 + B_1$
$\mathcal{C}_s$	$A'+$		$A' + A'$

FIG. 4. Descent in symmetry restricted to representations of the groups that are relevant to all possible configurations of three identical particles.

Tetrahedral shape in 16 Oxygen

Bijker, Iachello
PRL 112, 152501 (2014)

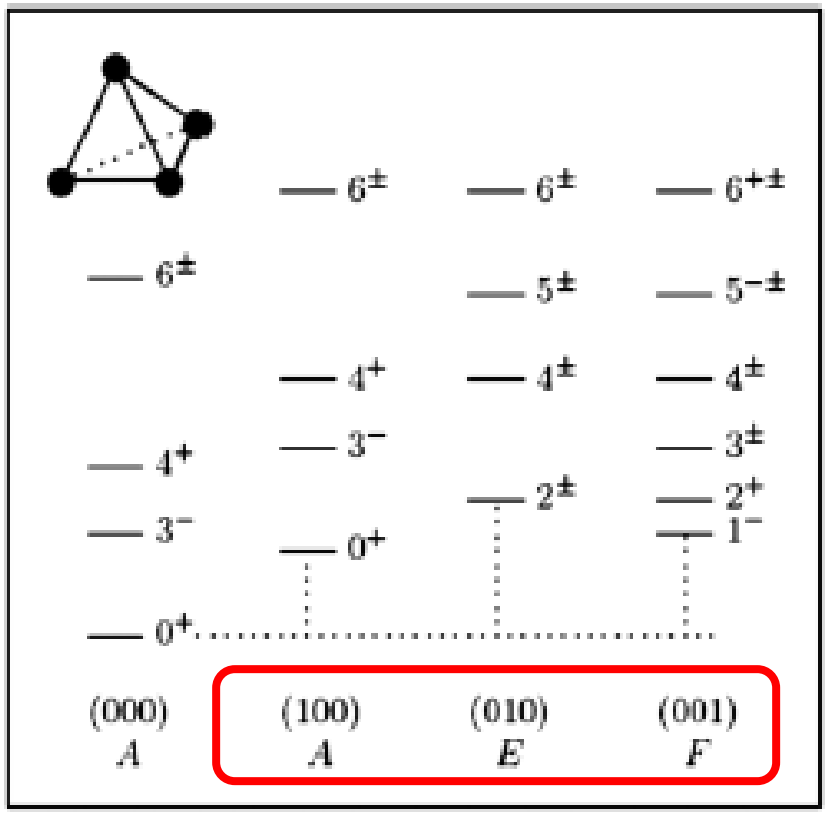

FIG. 1. Schematic spectrum of a spherical top with tetrahedral symmetry and $\omega_1 = \omega_2 = \omega_3$. The rotational bands are labeled by (v_1, v_2, v_3) (bottom). All states are symmetric under S_4.

What are the implication of the triangular structure in reactions?

PHYSICAL REVIEW C **101**, 014315 (2020)

Transition densities and form factors in the triangular α-cluster model of ^{12}C with application to $^{12}C + \alpha$ scattering

A. Vitturi,[1,2] J. Casal,[1,2] L. Fortunato,[1,2] and E. G. Lanza[3,4]
[1]*Dipartimento di Fisica e Astronomia "G. Galilei", Università di Padova*
[2]*I.N.F.N., Sez. di Padova, I-35131 Padova, Italy*
[3]*I.N.F.N., Sez. di Catania, I-95123 Catania, Italy*
[4]*Dipartimento di Fisica e di Astronomia "Ettore Majorana", Università Catania, Italy*

(Received 1 October 2019; published 21 January 2020)

Densities and transition densities are computed in an equilateral triangular α-cluster model for ^{12}C, in which each α particle is taken as a Gaussian density distribution. The ground state, the symmetric vibration (Hoyle state), and the asymmetric bend vibration are analyzed in a molecular approach and dissected into their components in a series of harmonic functions, revealing their intrinsic structures. The transition densities in the laboratory frame are then used to construct form factors and to compute distorted-wave Born approximation inelastic cross sections for the $^{12}C(\alpha, \alpha')$ reaction. The comparison with experimental data indicates that the simple geometrical model with rotations and vibrations gives a reliable description of reactions where α-cluster degrees of freedom are involved.

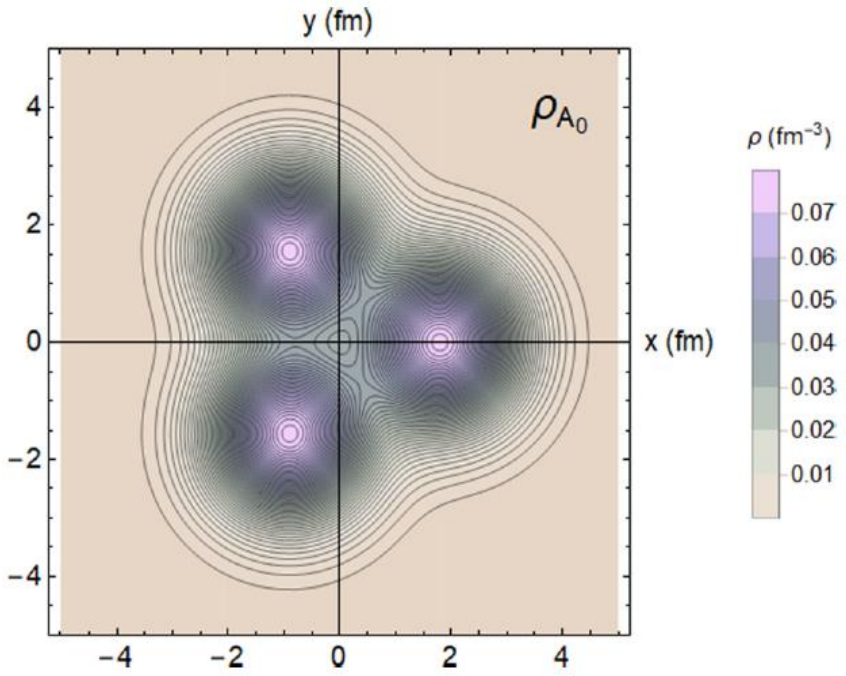

M. Kamimura, Nucl. Phys. A **351**, 456 (1981).
D. C. Cuong, D. T. Khoa, and Y. Kanada En'yo, Phys. Rev. C **88**, 064317 (2013).
M. Ito, Phys. Rev. C **97**, 044608 (2018).
Y. Kanada-En'yo and K. Ogata, Phys. Rev. C **99**, 064601 (2019).

Transition densities in 12C

In collaboration with A. Vitturi, E. Lanza and J. Casal

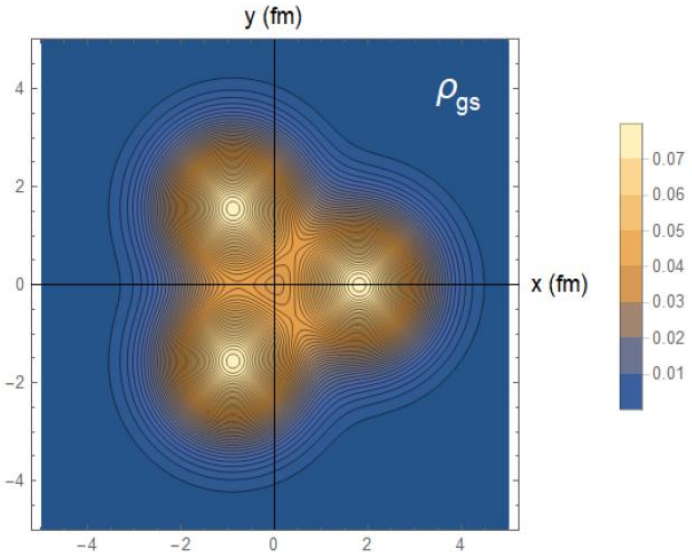

Ground state

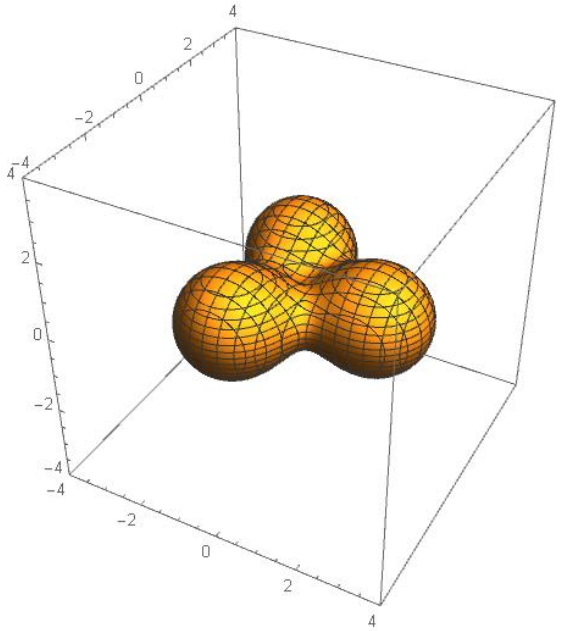

This model assume guassian densities for each alpha particle

$$\rho_\alpha(\vec{r}) = \left(\frac{\alpha}{\pi}\right)^{3/2} e^{-\alpha r^2}$$

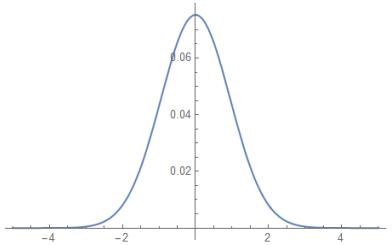

and a total density that is the sum of three displaced alpha's

$$\rho_{\rm gs}(\vec{r}, \{\vec{r}_k\}) = \sum_{k=1}^{3} \rho_\alpha(\vec{r} - \vec{r}_k),$$

which is then expanded in spherical harmonics

$$\rho_{\rm gs}(\vec{r}) = \sum_{\lambda\mu} \rho_{\rm gs}^{\lambda,\mu}(r) Y_{\lambda,\mu}(\theta, \varphi),$$

Ground and Hoyle bands

In collaboration with A. Vitturi, E. Lanza and J. Casal

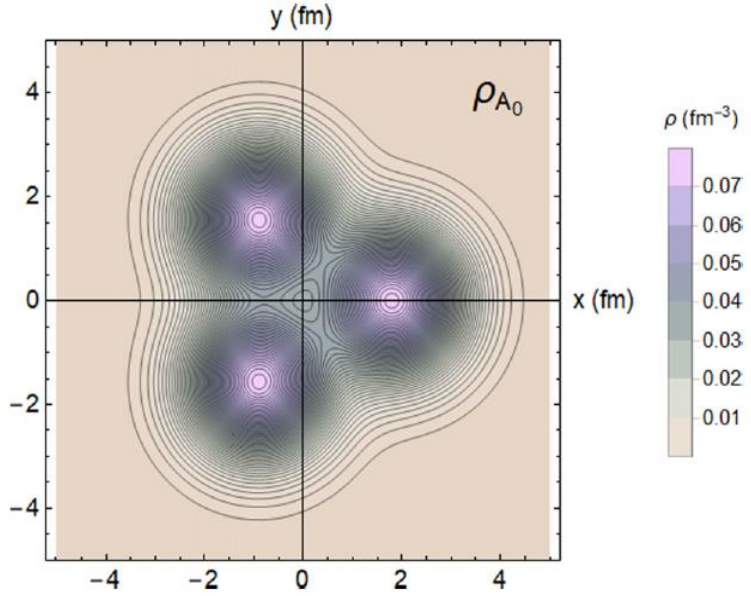

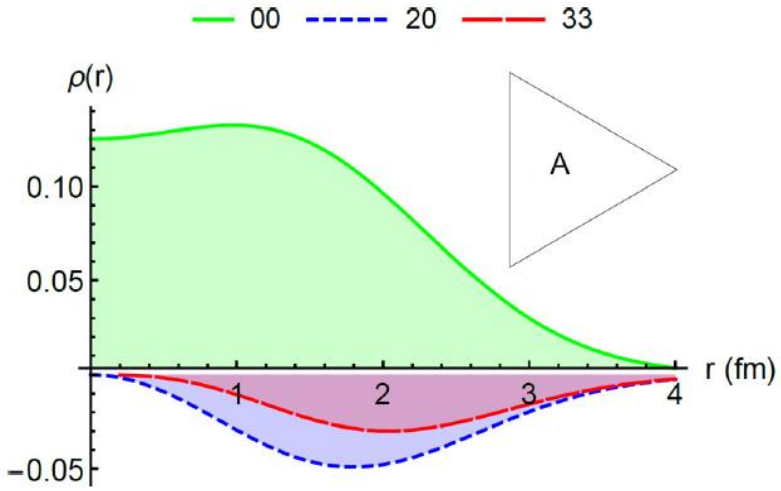

Ground state band

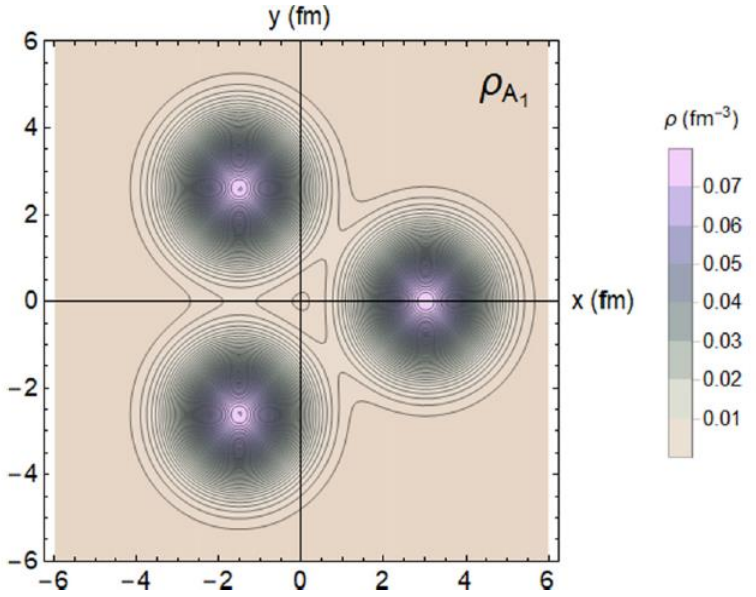

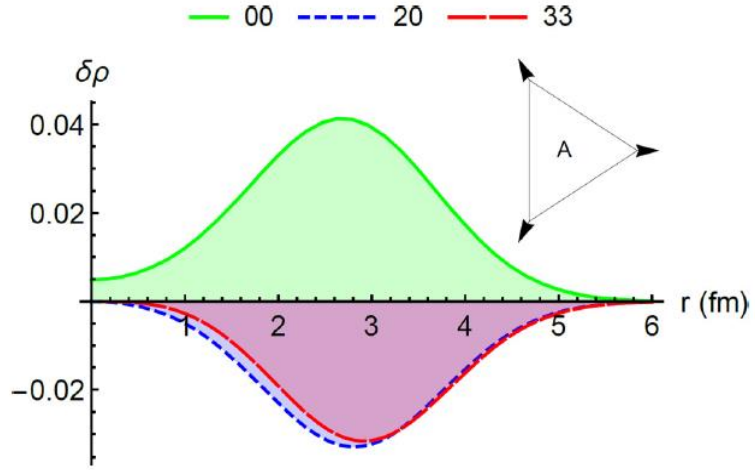

Hoyle state band

Parameters phenomenologically adjusted

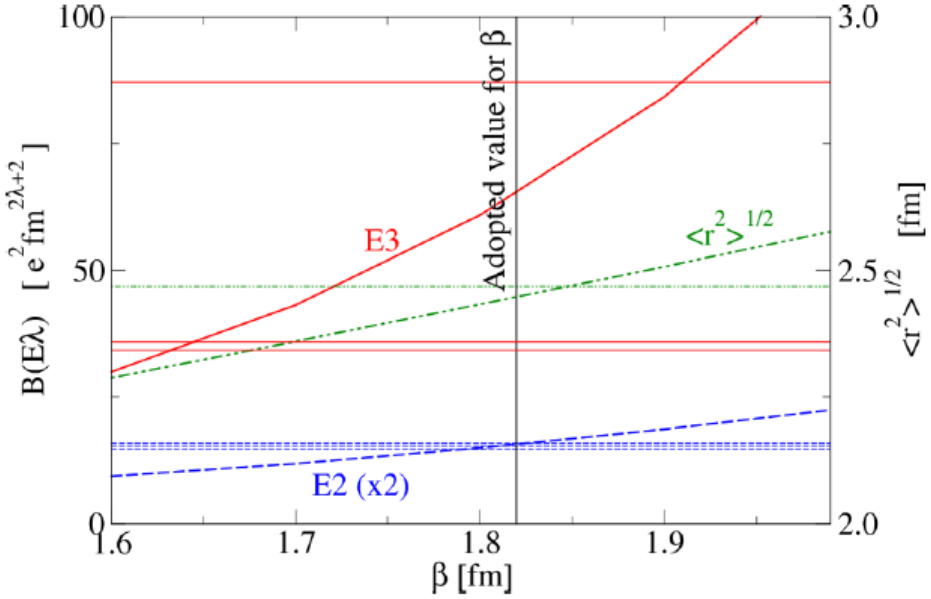

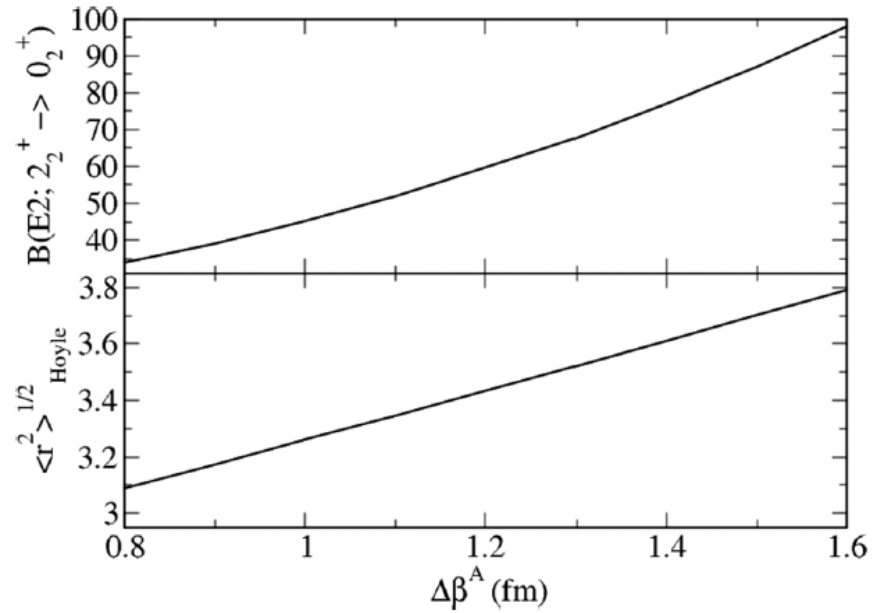

TABLE I. Calculated observables within the ground-state band.

$\langle r^2 \rangle^{1/2}_{0_1^+}$	2.45 (fm)
$B(E2; 2_1^+ \rightarrow 0_1^+)$	7.86 (e^2 fm^4)
$B(E3; 3_1^- \rightarrow 0_1^+)$	65.07 (e^2 fm^6)
$B(E4; 4_1^+ \rightarrow 0_1^+)$	96.99 (e^2 fm^8)

TABLE II. Quantities calculated in the present work for the Hoyle band using the values of β and χ_1 given in the text.

$\langle r^2 \rangle^{1/2}_{0_2^+}$	3.44 (fm)
$B(E2; 2_2^+ \rightarrow 0_1^+)$	0.58 (e^2 fm^4)
$B(E2; 0_2^+ \rightarrow 2_1^+)$	2.90 (e^2 fm^4)
$B(E3; 3_2^- \rightarrow 0_1^+)$	70.42 (e^2 fm^6)
$M(E0; 0_2^+ \rightarrow 0_1^+)$	5.4 (e fm^2)

Transition densities in 12C

A-band

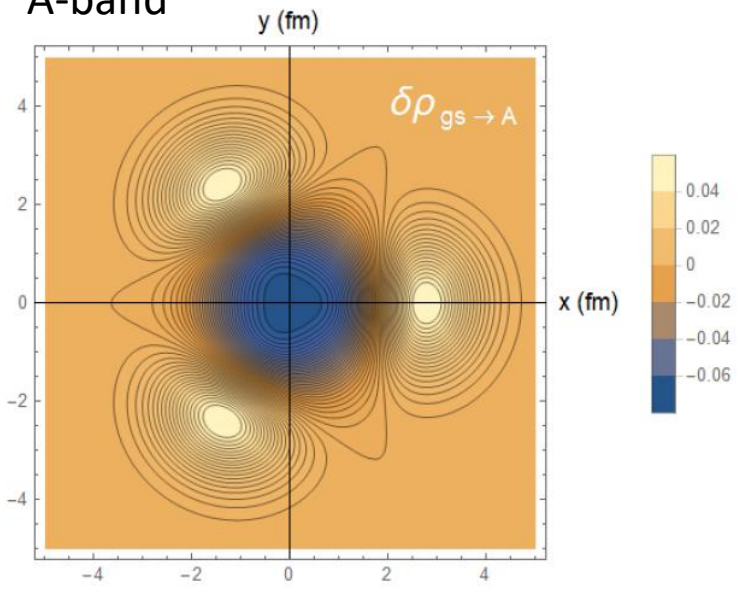

FIG. 7: Transition density for the first A-type vibration.

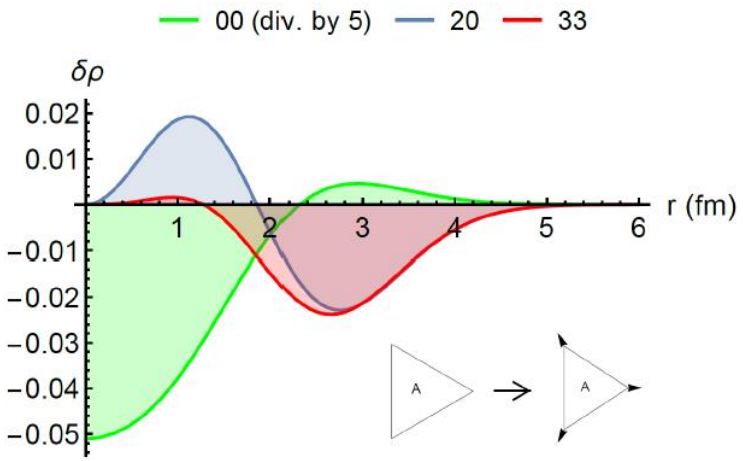

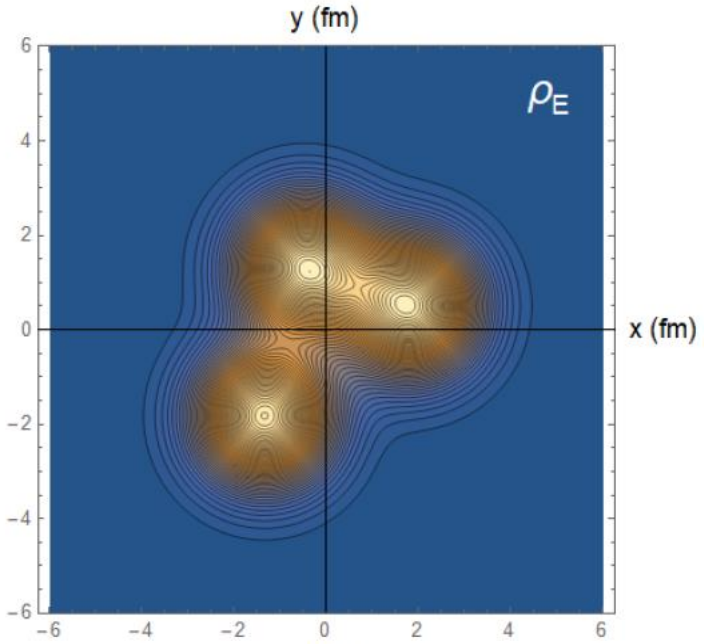

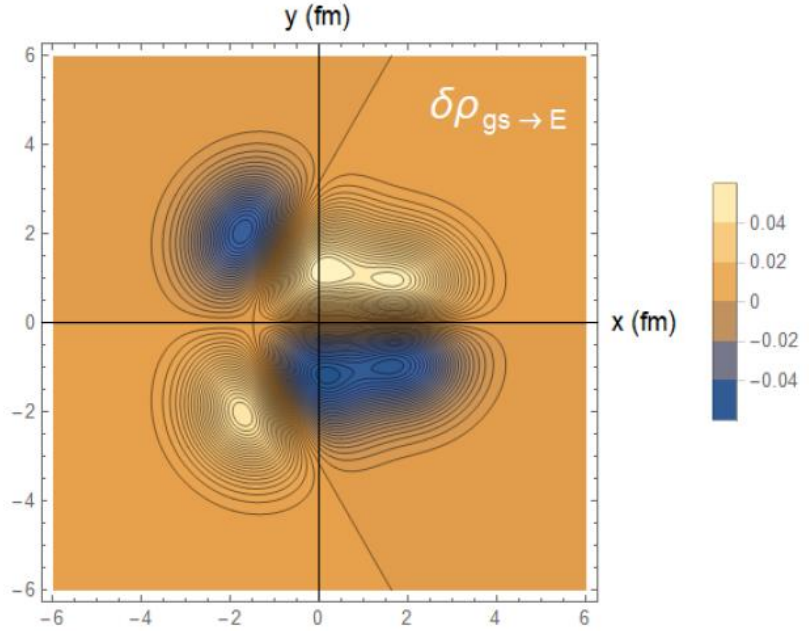

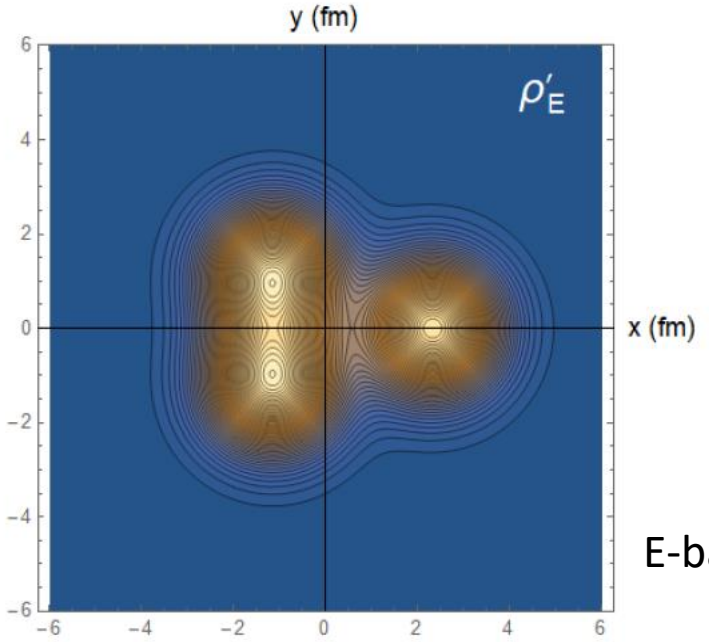

E-band

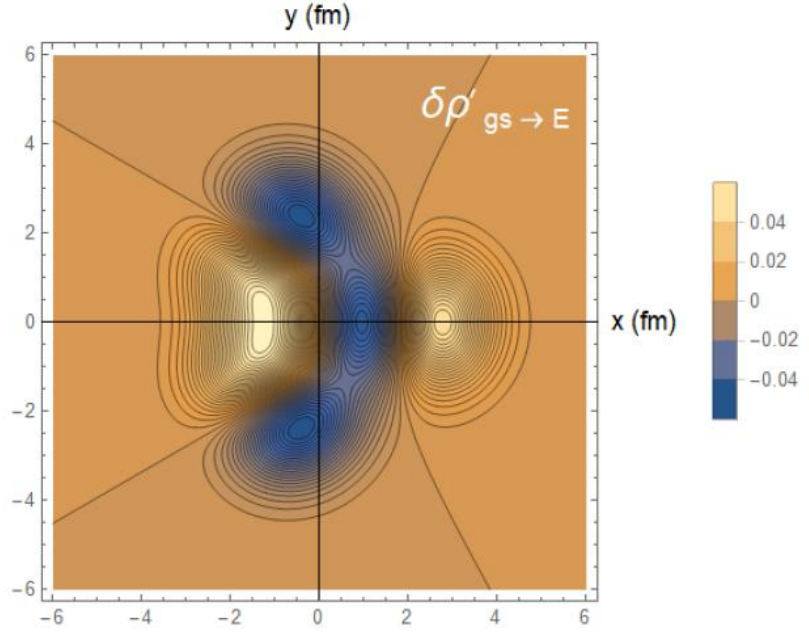

Transition densities -> Form Factors -> Coupled Channels -> Cross-sections

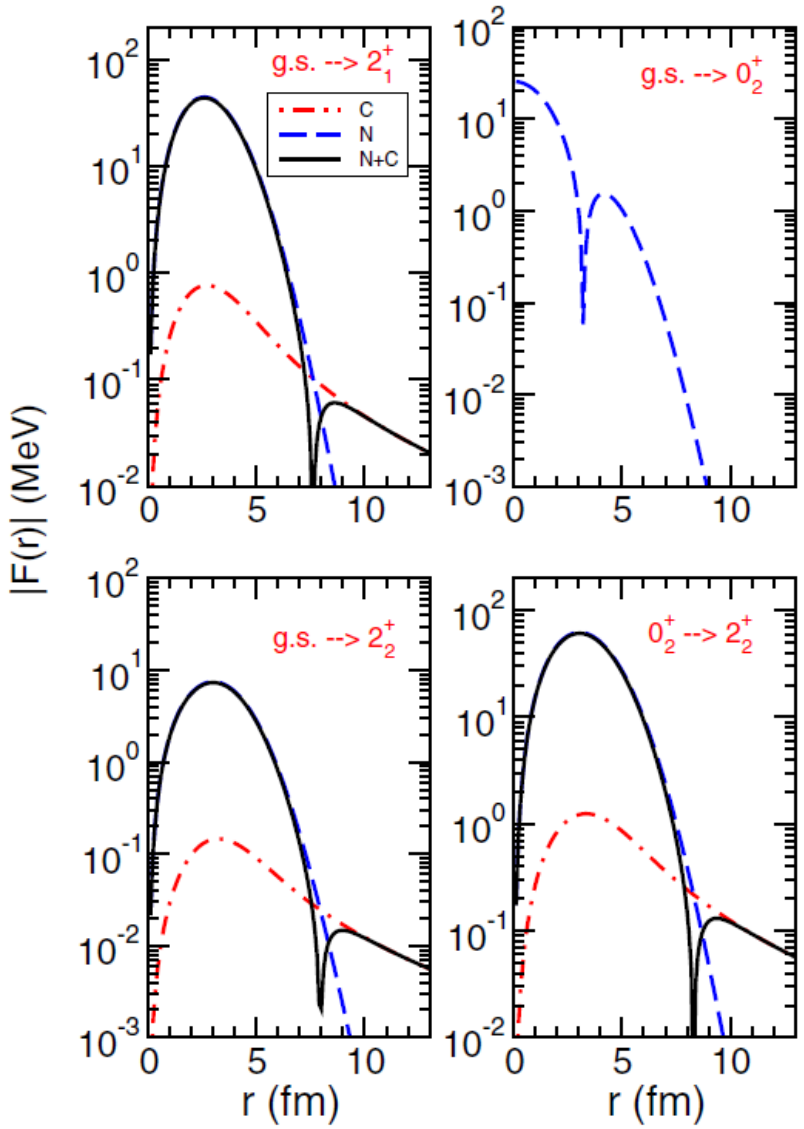

FIG. 15. Form factors in logarithmic scale for a few inelastic excitation processes of interest. We show the nuclear, Coulomb, and total form factors.

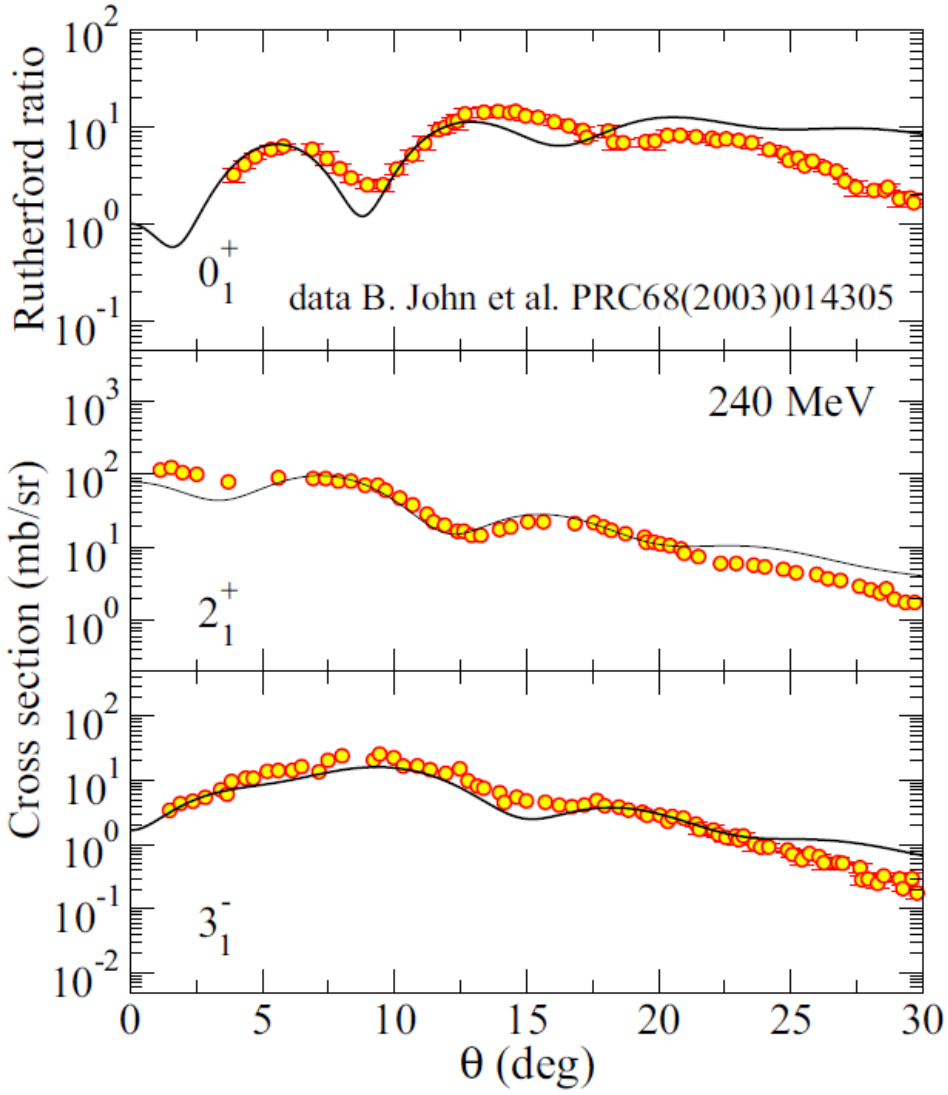

FIG. 16. Differential cross section for the elastic scattering and the transitions $0^+_1 \rightarrow 2^+_1$ and $0^+_1 \rightarrow 3^+_1$ at 240-MeV bombarding energy. Data are from Ref. [41] (retrieved through EXFOR).

Lots of results that I dont'have time to discuss in details.
They confirm that with just a simple triangular model one catches all the gross features, not only of the nuclear structure, but also of reaction dynamics of 12C.

Importance of the imaginary part of the ion-ion potential

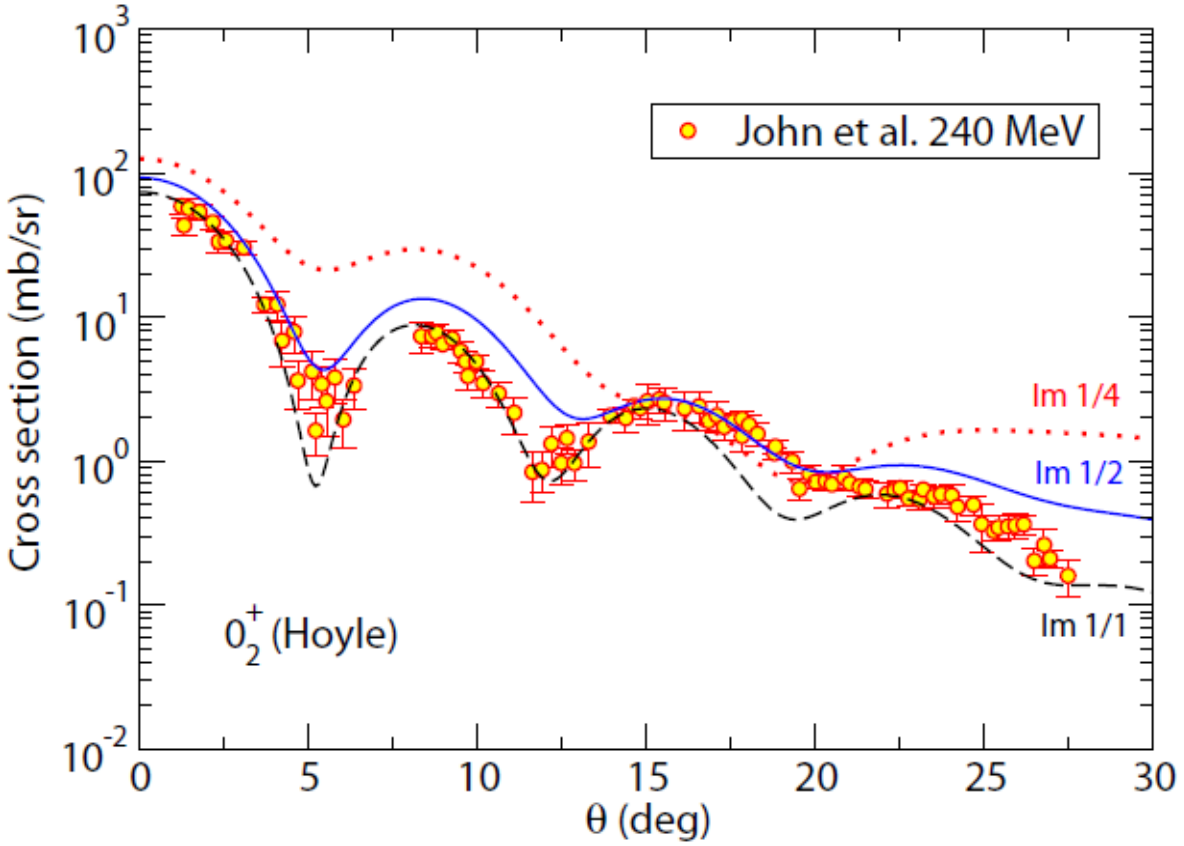

FIG. 17. Differential cross section for the transition $0_1^+ \rightarrow 0_2^+$ at 240-MeV bombarding energy. Data are from Ref. [41] (retrieved through EXFOR) and the three curves have different factors for the depth of the imaginary part as indicated in the figure.

V(r) + iW(r)

Extended to 16O in a tetrahedral arrangement

Eur. Phys. J. A (2021) 57:33

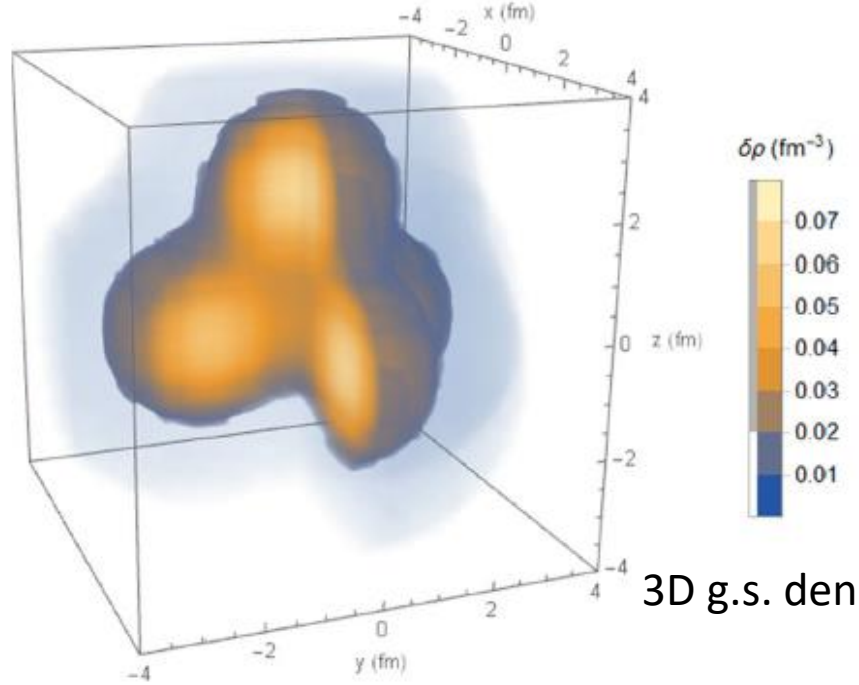

3D g.s. density plot

Eur. Phys. J. A (2021) 57:33
https://doi.org/10.1140/epja/s10050-021-00347-5

THE EUROPEAN PHYSICAL JOURNAL A

Regular Article - Theoretical Physics

Alpha-induced inelastic scattering and alpha-transfer reactions in ^{12}C and ^{16}O within the Algebraic Cluster Model

Jesus Casal[1,2], Lorenzo Fortunato[1,2], Edoardo G. Lanza[3,4], Andrea Vitturi[1,2,a]

The tetrahedral group Td allows for singly- , doubly- and triply-degenerate representations

→ one can see all of these excitation modes in the spectrum of 16O !

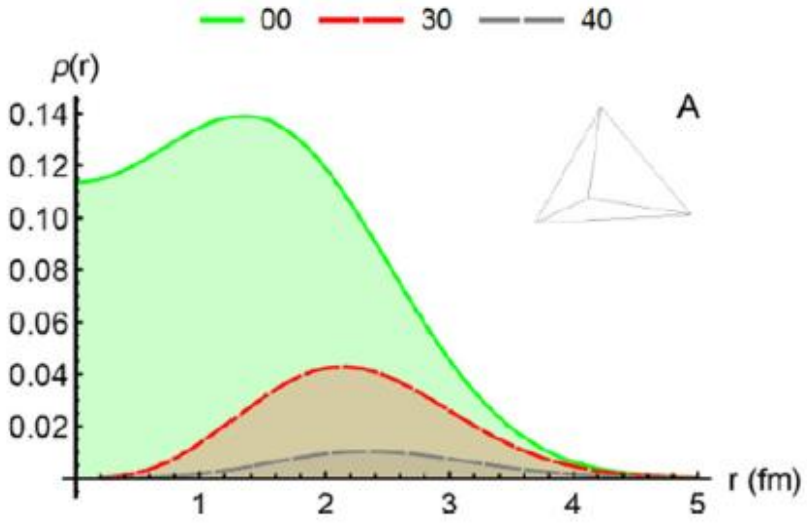

Expansion in spherical harmonics

Extended to 16O in a tetrahedral arrangement -> 12C(α,γ)16O

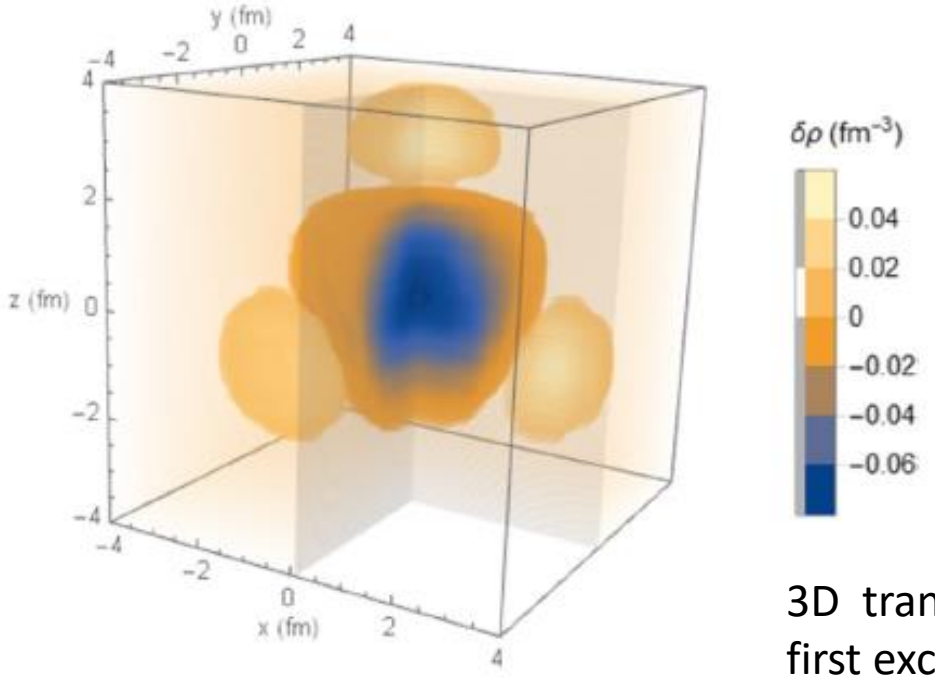

3D transition density to first excited A band (0+)

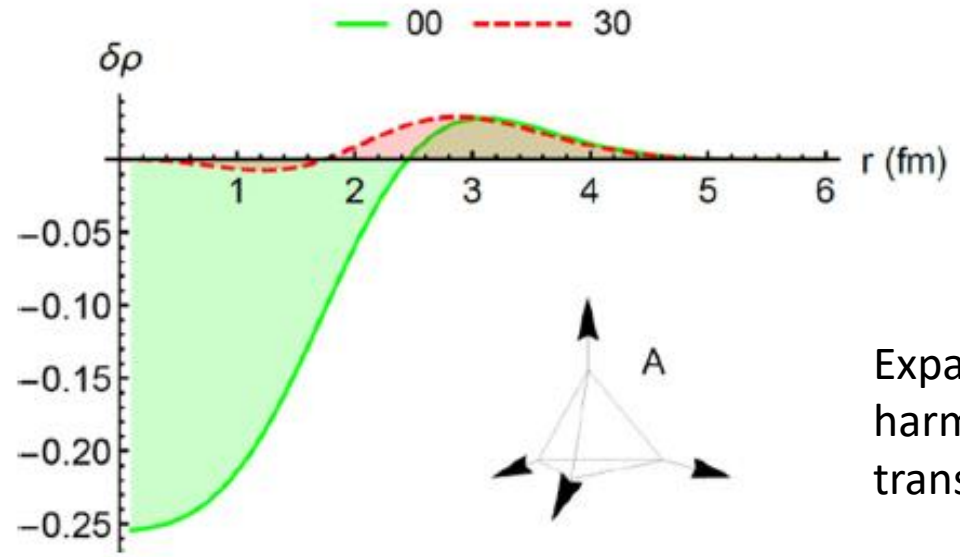

Expansion in spherical harmonics of the transition densities

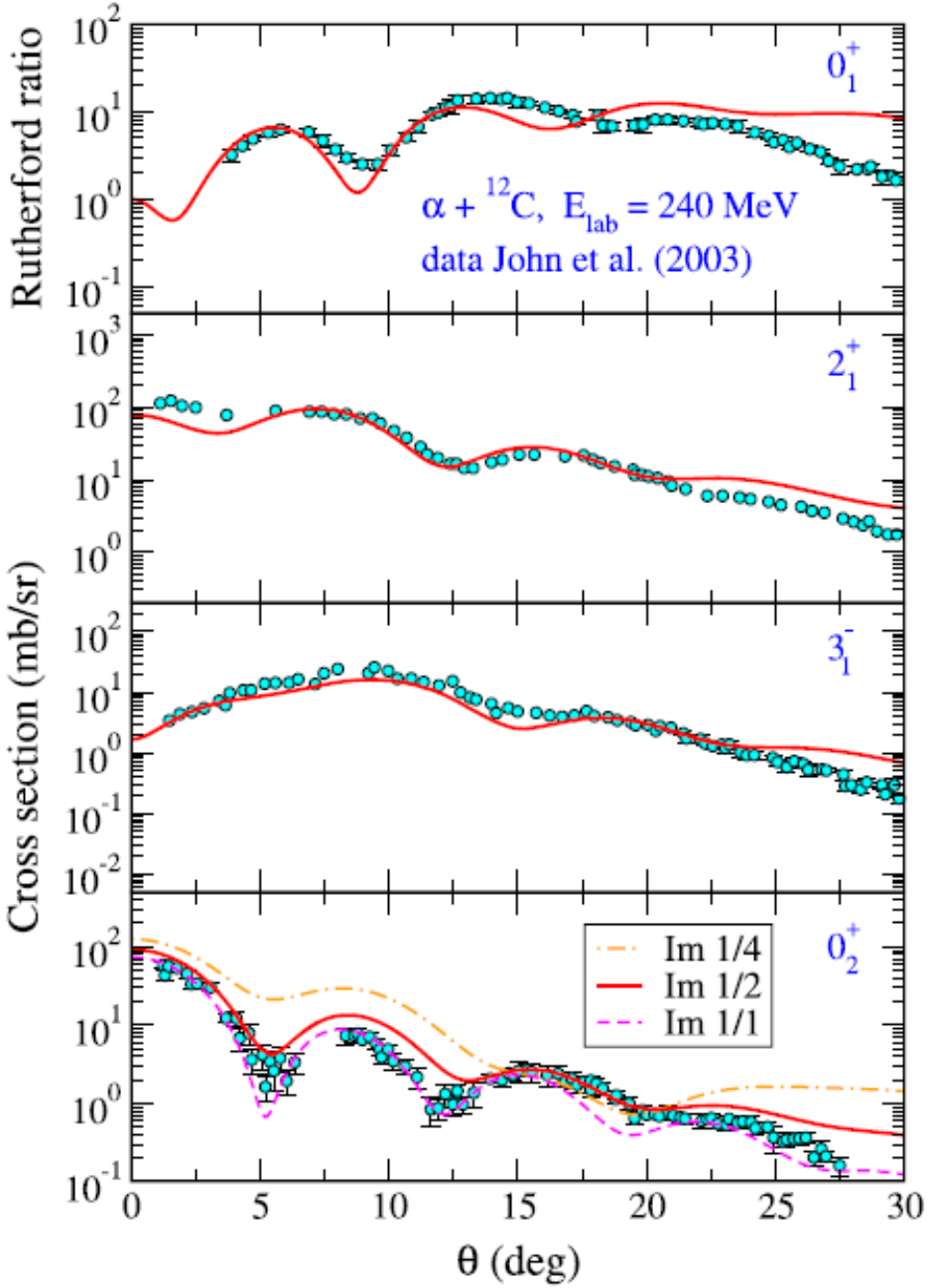

Selection rule for alpha transfer

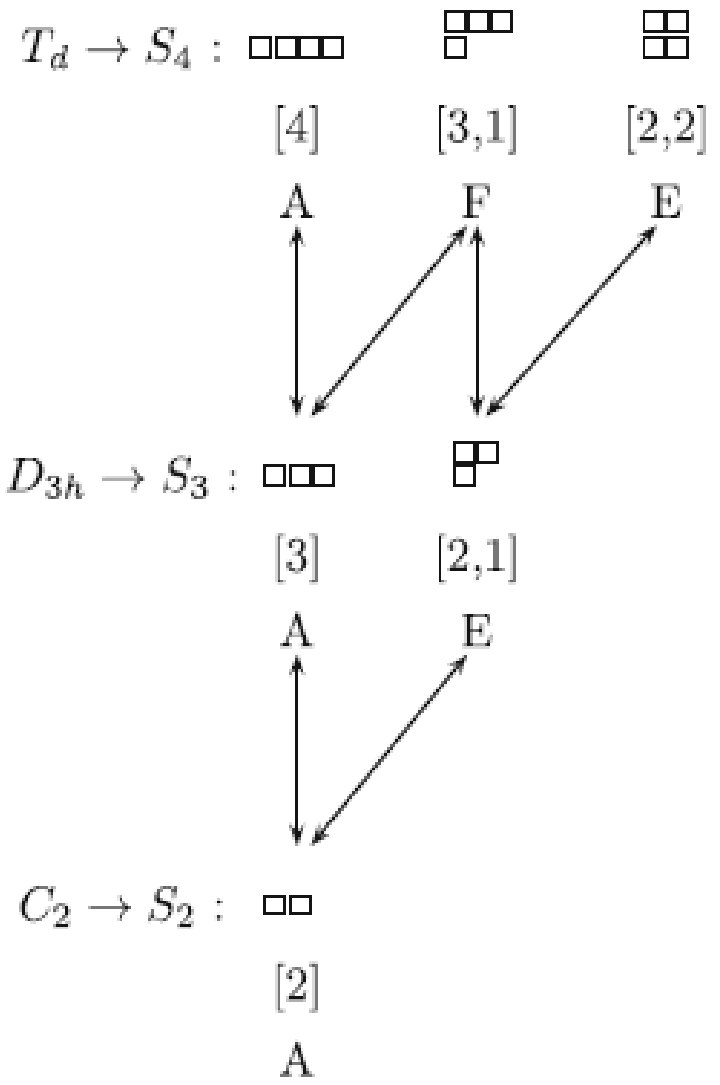

Fig. 8 The representations of the systems with 4,3 and 2 α particles connected by arrows corresponding to processes of induction/restriction that amounts to the addition/removal of one box from the corresponding Young diagrams

Taking into account the symmetric groups of 2-3-4 identical objects, one can up with a scheme for alpha-transfer (I mean the addition or removal of 1 alpha particle) based on Young tableaux, i.e. on the representations of those groups.

It turns out that not all of them can be connected, for instance one cannot go from the A states of 12C to the E states of oxygen, the alpha transfer should be identically zero !

Fluorine-29 stands on the coast of the island of inversion

COMMUNICATIONS PHYSICS

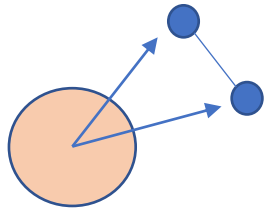

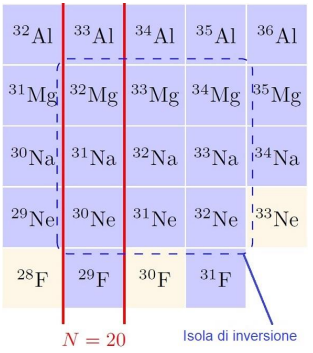

PERSPECTIVE

https://doi.org/10.1038/s42005-020-00402-5 OPEN

The ^{29}F nucleus as a lighthouse on the coast of the island of inversion

L. Fortunato [1,2]✉, J. Casal [1,2], W. Horiuchi [3], Jagjit Singh [4] & A. Vitturi[1,2]

Fluorine-29 stands on the coast of the island of inversion

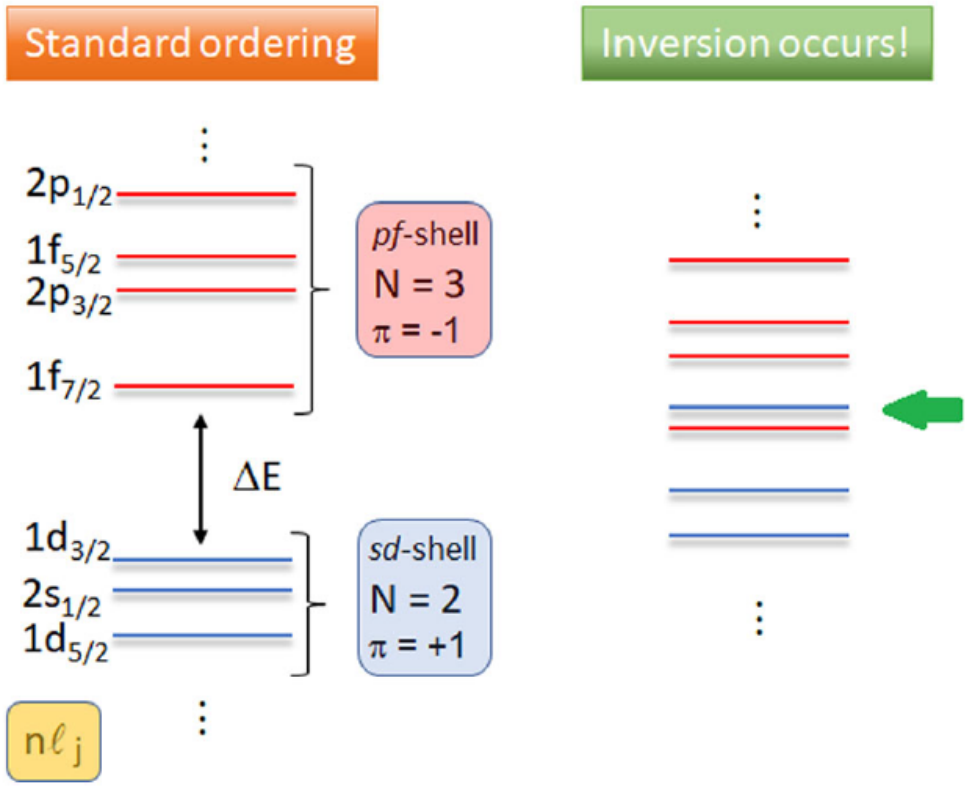

Fig. 1 Standard ordering of shell-model energy levels and typical inversion mechanism. The $N=2$ *sd*-shell and the $N=3$ *pf*-shell with positive and negative parity π, respectively, are shown on the left in the standard ordering (states are labeled by the standard set of quantum number $n\ell_j$). Inversion occur (right) when the shell gap, ΔE, associated with the filling of 20 neutrons, disappears and one level (or more) of the $N=3$ *pf*-shell gets lower than one (or more) of the levels of the $N=2$ *sd*-shell.

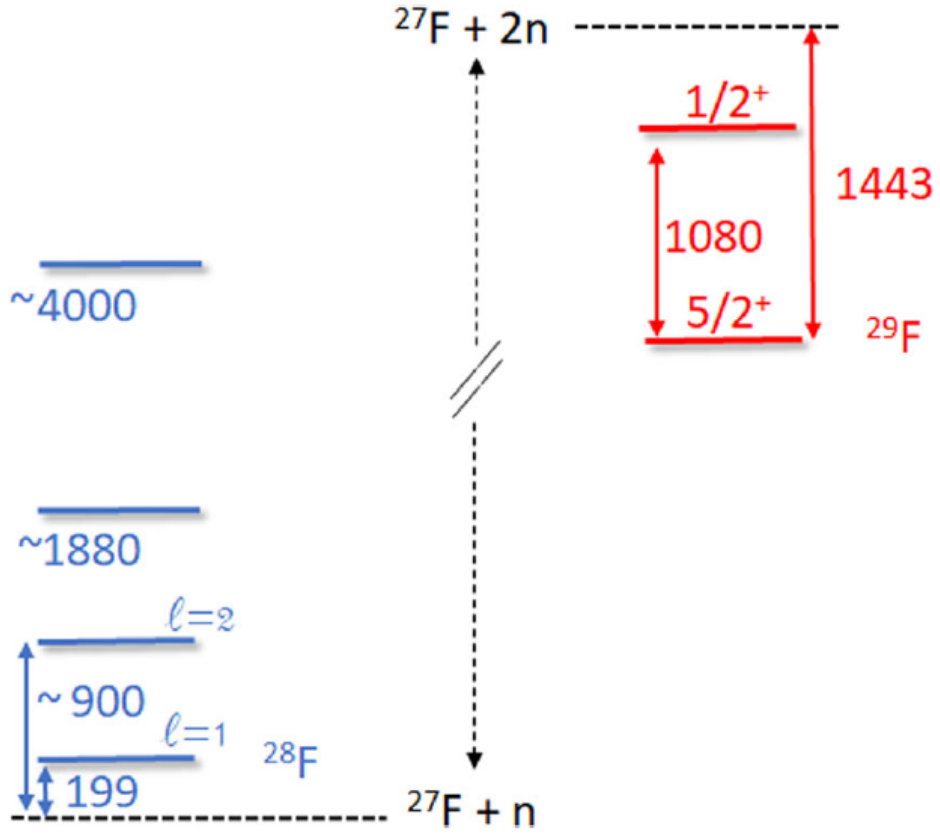

Fig. 2 Synopsis of known experimental data on ^{28,29}F. All energies are in keV (not to scale) from refs. [4 --6,11]. States in red are labelled by the J^π quantum numbers and energies are referred to the ^{27}F + 2n threshold. States in blue are inferred from the ^{29}F(−1n) column of Fig. 2 of ref. [6], and correspond only to the states decaying to the ground state of ^{27}F. They are labelled by the orbital angular momentum quantum number, ℓ, when available. Energies are referred to the ^{27}F + n threshold.

Fluorine-29 stands on the coast of the island of inversion

We had previously PRC **101**, 024310 (2020) proposed 4 scenarios for the structure of the very exotic nucleus 29F, called A,B,C,D , based on the three-body hyperspherical formalism by J.Casal

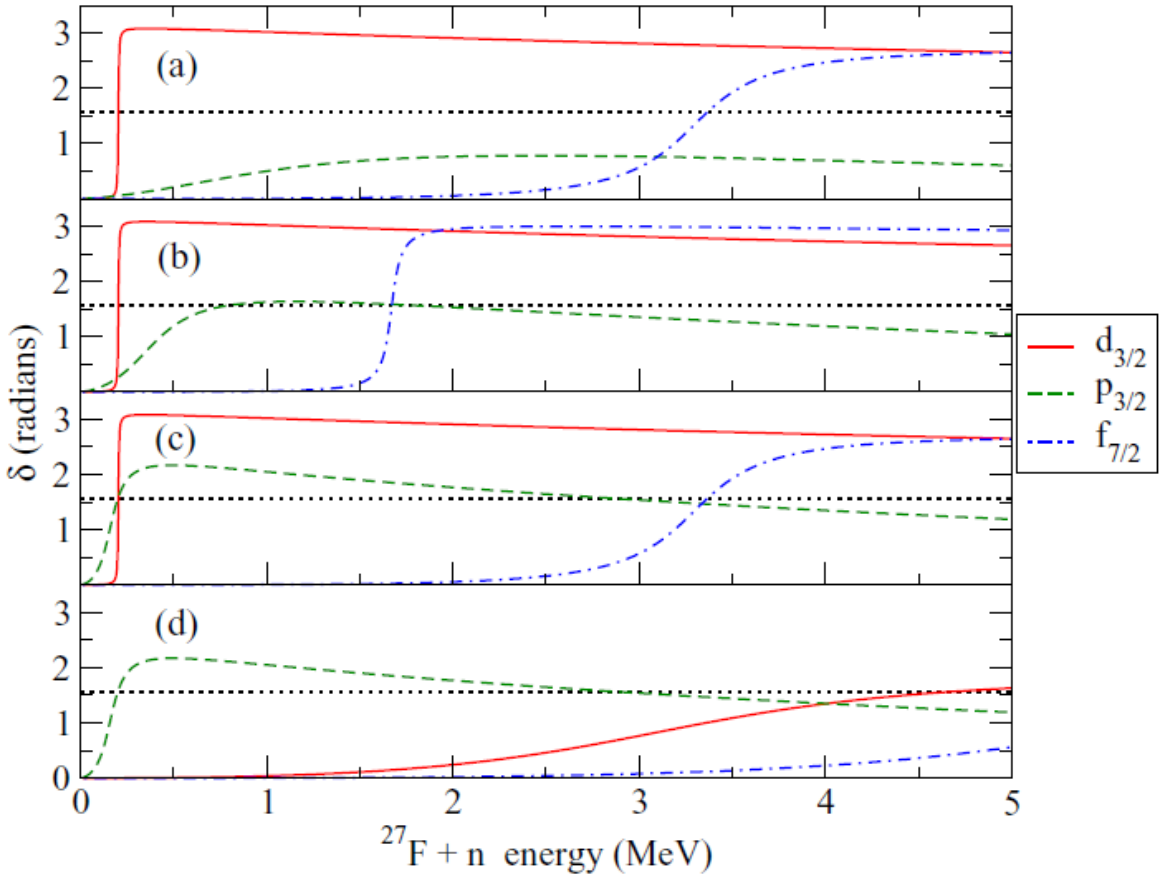

FIG. 1. ^{27}F $+n$ phase shifts for $d_{3/2}$, $p_{3/2}$, and $f_{7/2}$ states, corresponding to different sets (A–D). The dotted black line corresponds to $\pi/2$.

Standard

Intruder

Degenerated

Inverted

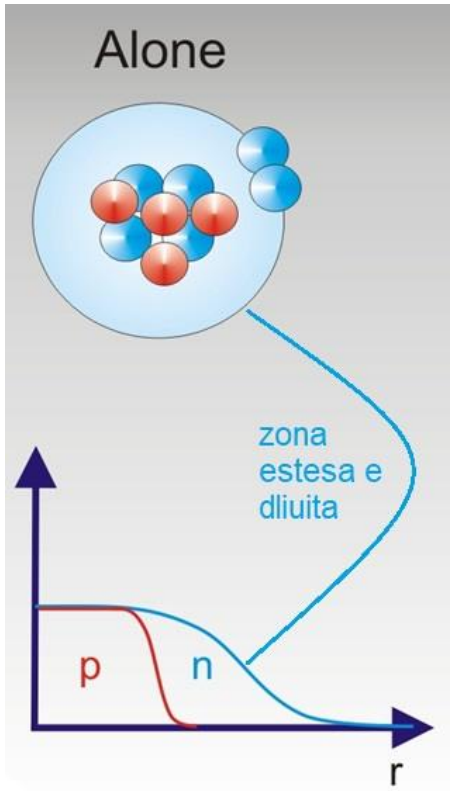

Fluorine-29 stands on the coast of the island of inversion

New experiments by
1) Revel, A. et al. "Extending the southern shore of the island of inversion to 28F" PRL 124, 152502 (2020)
and then
2) Bagchi, S. et al. "Two-neutron halo is unveiled in 29F" PRL 124, 222504 (2020)

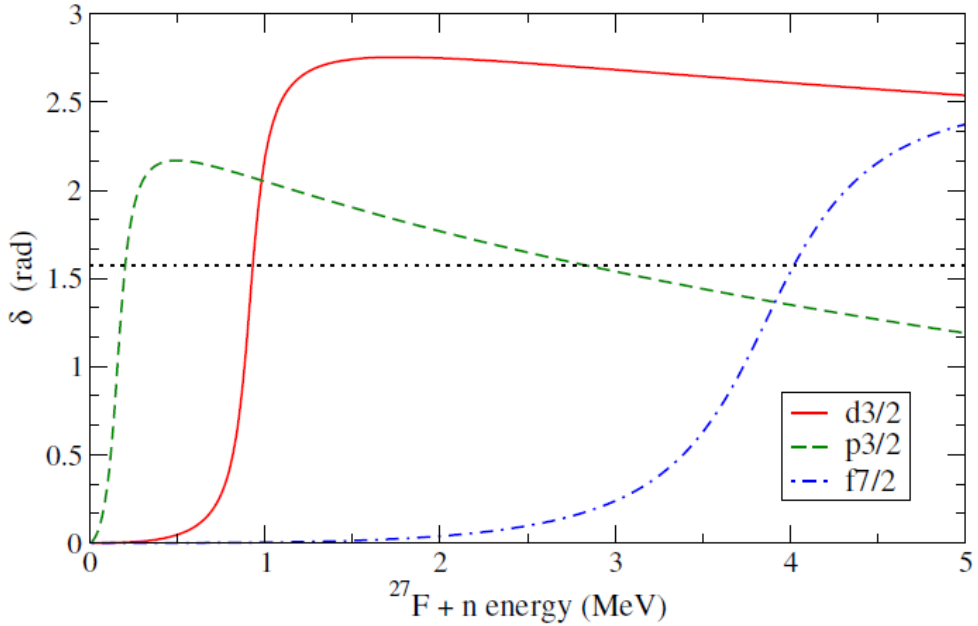

Fig. 3 Phase-shifts, δ, for the ^{27}F + n system in the D$^{\flat}$ scenario as a function of the neutron-core relative energy. Adjusting the red curve to reproduce the *d*-resonance at about 0.9 MeV, also gives the *f*-wave state (blue curve) at about 4 MeV.

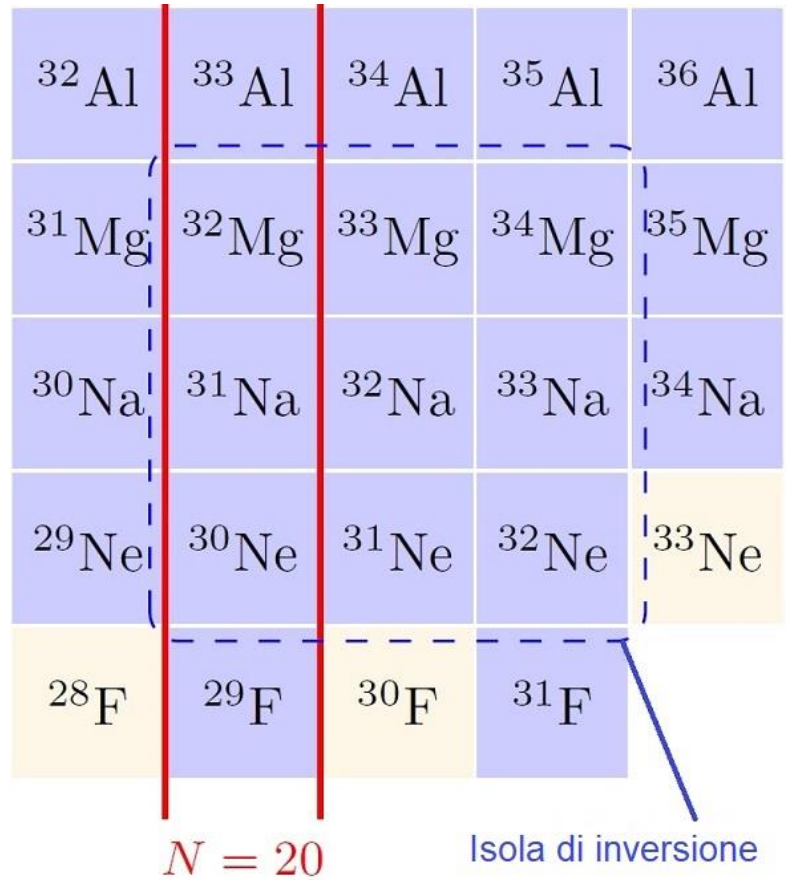

Final picture … Scenario D ♭

Fluorine-29 stands on the coast of the island of inversion

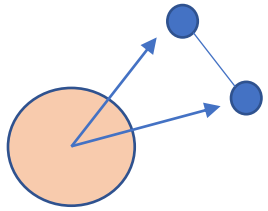

$$\frac{d\sigma}{d\varepsilon} = (\alpha Z_2)^2 \sum_{\pi\lambda\mu} \left(\frac{\Delta E}{\hbar c}\right)^{2\lambda-2} \frac{dB}{d\varepsilon}(\pi\lambda; \mathrm{gs} \rightarrow \mathrm{Cont.}) |G_{\pi\lambda\mu}(\beta^{-1})|^2 g_\mu(\xi)$$

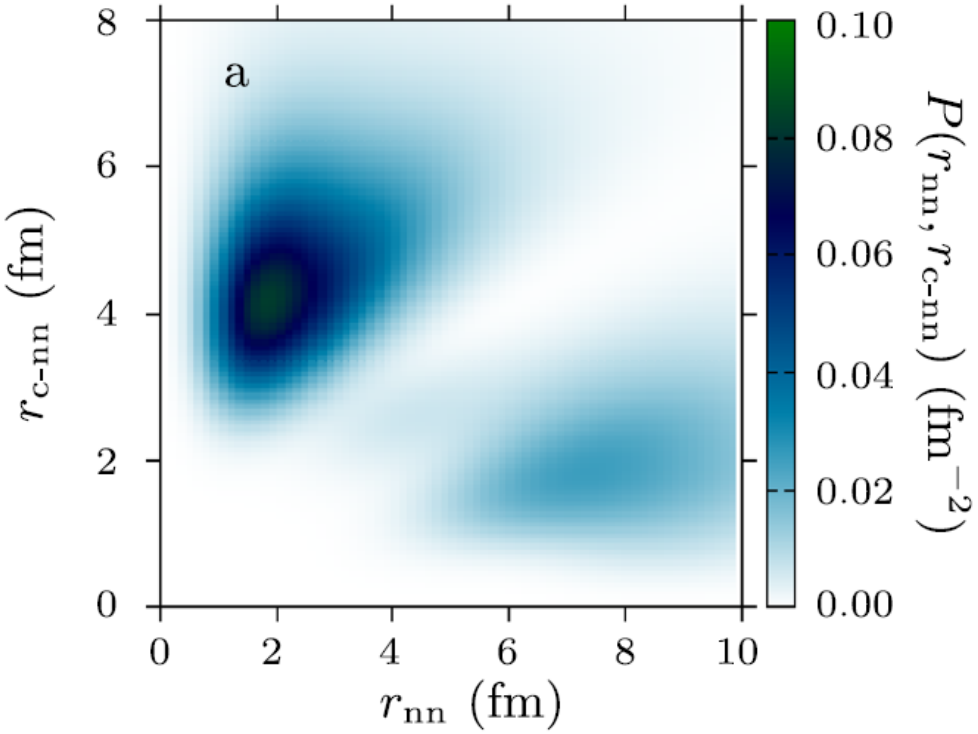

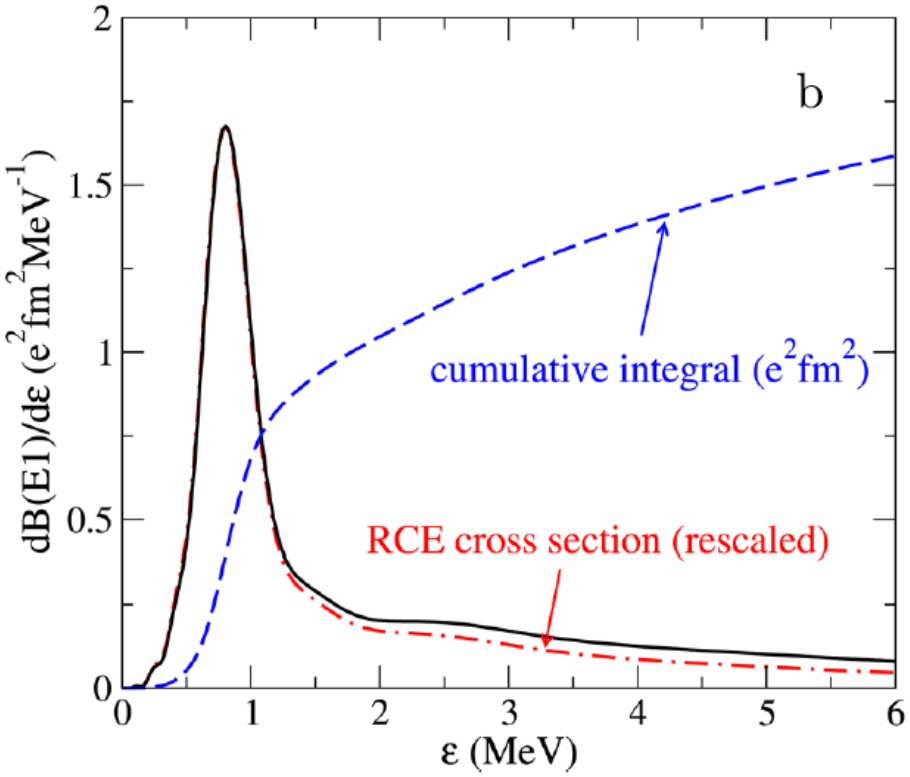

Fig. 4 Results on ^{29}F within the new D^b scenario. a Ground-state probability density of ^{29}F as a function of the distance between the two valence neutrons (r_{nn}) and that between their center of mass and the core (r_{c-nn}). The maximum probability density corresponds to the dineutron configuration. **b** Electric dipole ($E1$) strength function from the ground state to continuum as a function of the ^{27}F + n + n energy. The dashed line indicates the cumulative integral. The dash-dotted line is the corresponding Relativistic Coulomb Excitation (RCE) cross-section, scaled to the same maximum to illustrate the decreasing proportionality with the energy.

Summary

- ✓ **PRC 99 (2019)** I have suggested to use the highly polarized monochromatic gamma rays that will be available at ELI-NP as a tool to study the molecular vibrations of clusterized nuclei, taking as a definite example the 12C nucleus as composed of 3 α particles. A measure of depolarization ratio could be done in a sort of Raman nuclear fluorescence experiment. This would yield precise patterns of vibrational spectra, that will correlate directly with a given geometric configuration possessing a discrete point-group symmetry.

- ✓ **PRC 101, 014315 (2021)** We have calculated transition densities and form factors for 12C in a triangular molecular model for the g.s., A and E bands. We applied this model to 12C+ α scattering showing a very good agreement.
- ✓ **EPJA 57 (2021)** We have extended these results to 16O in a tetrahedral arrangement and we have calculated alpha-induced reaction observables. I have found a new selection rule for alpha-transfer based on group theory.

- ✓ **Comm.Physics 3 (2020)** and also **PRC 101, 024310 (2020)** We have succesfully interpreted new experimental results on the structure of 29F indicating it lies at the border of the island of inversion.

800 1222·2022 ANNI
UNIVERSITÀ DEGLI STUDI DI PADOVA
Dipartimento di Fisica e Astronomia Galileo Galilei
INFN Istituto Nazionale di Fisica Nucleare

A few points for discussion

- if the g.s. rotational band contains the same multipolarity that one is trying to excite in the vibrational bands, this is also to be included in the above patterns.

- in principle the degree of polarization might be close to 3/4 also for polarized (A) bands, therefore it might become hard to distinguish between them

- non-cluster degrees of freedom might come into play at a certain energy, thus blurring the picture

- in nuclei with a cluster structure including *t* or *h* clusters, the interplay with single-particle orbits around a molecular center might also be very relevant

- I guess a BEC gas would show no geometric arrangments (no equilibirum points) and would behave as an L=0 state (a sphere), thus offering only 1 such bands of A type (polarized).

A word of caution

DISCLAIMER for the first topic:

- It is perfectly clear to us that molecular models of nuclei are FUNDAMENTALLY DIFFERENT from molecular physics, where the Born-Oppenheimer approximation is valid and one can think of nuclear motion as a small vibration, happening only close to the minimum of a very deep potential energy surface (in molecular energy scales).

- Nuclei have large kinetic energy <T>, comparable to the potential energy <V> and the zero point motion inside the P.E.S. is a large fraction of the well depth, therefore there are LARGE FLUCTUATIONS around the equilibrium points and we SHOULD NOT EXPECT that the vibrational levels are deeply lying in the potential well, at most they can be weakly bound states, close to threshold, or more probably resonances in the continuum!

- Dispite this, it is instructive to look at
  1. the normal modes, i.e. the «best» internal coordinates
  2. symmetry-adapted vibrational orbitals
  3. the energy scale and structure of the vibrational levels

Nomenclature

Table II: The Mulliken symbols used to describe the symmetry species of point groups including their meaning with respect to molecular symmetry

Mulliken Symbols of Symmetry Species (Column 1 In Character Table)	Meaning
A	Symmetric with respect to principal axis of symmetry
B	Antisymmetric with respect to principal axis of symmetry
E	Doubly degenerate, two-dimensional irreducible representation
T	Triply degenerate, three-dimensional irreducible representation
g	Symmetric with respect to a center of symmetry
u	Antisymmetric with respect to a center of symmetry
1 (subscript)	Symmetric with respect to a C_2 axis that is perpendicular to the principal axis. Where there is no such axis the subscript indicates that reflection in a $_v$ plane of symmetry is symmetric.
2 (subscript)	Antisymmetric with respect to a C_2 axis that is perpendicular to the principal axis. Where there is no such axis the subscript indicates that reflection in a $_v$ plane of symmetry is antisymmetric.
′ (prime)	Symmetric with respect to reflection in a horizontal plane of symmetry
″ (double prime)	Antisymmetric with respect to reflection in a horizontal plane of symmetry

From D. Tuschel – Spectroscopy : Molecular Spectroscopy workbench (2014)

Tetrahedral shape in 16 Oxygen

They use a somewhat simplified notation based on the permutation (sub)groups S_3 and S_4 of the full discrete groups D_{3h} and T_d respectively , but the essence is the same.

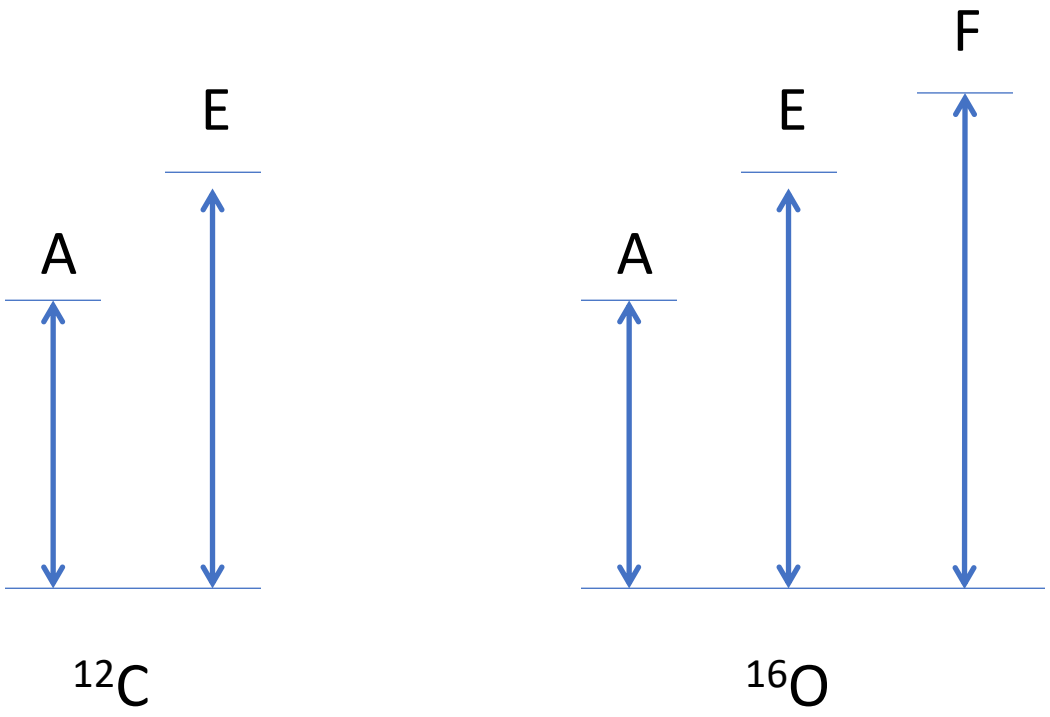

Tables for 2 clusters and for 3 clusters of type AAB

name	shape	group	Γ_{vib}	Patterns
linear AA		$\mathcal{D}_{\infty h}$	A_{1g}	
linear AB		$\mathcal{C}_{\infty\nu}$	A_1	

name	shape	group	Γ_{vib}	Patterns
linear ABA		$\mathcal{D}_{\infty h}$	$A_{1g} + A_{1u} + E_{1u}$	
linear AAB		$\mathcal{C}_{\infty\nu}$	$2A_1 + E_1$	
isosceles AAB	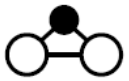	$\mathcal{C}_{2\nu}$	$2A_1 + B_1$	
scalene AAB	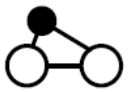	$\mathcal{C}_s$	$3A'$	

Tables for 4clusters, only some have been worked out

name	shape	group	Γ_{vib}	Patterns
linear aaa		$\mathcal{D}_{\infty h}$	$2A_{1g} + E_{1g} + E_{4g} + A_{1u} + E_{1u}$	2/6
linear aba		$\mathcal{D}_{\infty h}$	$2A_{1g} + E_{1g} + A_{1u} + E_{1u}$	2/5
square a^4b^2		$\mathcal{D}_{4h}$	$A_{1g} + B_{1g} + B_{2g} + B_{2u} + E_u$	1/5
kite a^4bc		$\mathcal{D}_{2h}$	$2A_g + B_{1g} + B_{1u} + B_{2u} + B_{3u}$	2/6
centered eq. triangle a^3b^3		$\mathcal{D}_{3h}$	$A_1' + 2E' + A_2''$	1/4
rectangle $a^2b^2c^2$		$\mathcal{D}_{2h}$	$2A_g + B_{1g} + A_u + B_{2u} + B_{3u}$	2/6
tetrahedron a^6		$\mathcal{T}_d$	$A_1 + E + T_2$	1/3
uneq. tetrah. a^3b^3		$\mathcal{C}_{3\nu}$	$2A_1 + 2E$	2/4
wedge a^4b^2		$\mathcal{D}_{2d}$	$2A_1 + B_1 + B_2 + E$	2/5
2 triangles at 90^o a^5b		$\mathcal{C}_{2\nu}$	$3A_1 + A_2 + B_1 + B_2$	3/6

One might gather information on polarization due to alpha particles' substructures